

PLEASE RETURN TO
MFC BRANCH LIBRARY

INL Technical Library

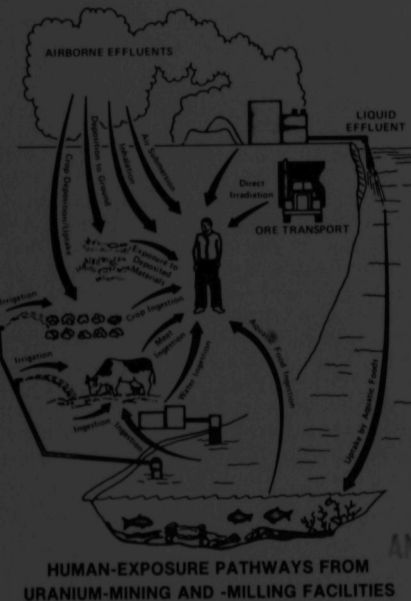


146407

ANALYSIS OF THE GAMMA SPECTRA OF THE URANIUM, ACTINIUM, AND THORIUM DECAY SERIES

by

Michael H. Momeni



PROPERTY OF
ANL-W Technical Library



ARGONNE NATIONAL LABORATORY, ARGONNE, ILLINOIS

Prepared for the U. S. DEPARTMENT OF ENERGY

The facilities of Argonne National Laboratory are owned by the United States Government. Under the terms of a contract (W-31-109-Eng-38) among the U. S. Department of Energy, Argonne Universities Association and The University of Chicago, the University employs the staff and operates the Laboratory in accordance with policies and programs formulated, approved and reviewed by the Association.

MEMBERS OF ARGONNE UNIVERSITIES ASSOCIATION

The University of Arizona	The University of Kansas	The Ohio State University
Carnegie-Mellon University	Kansas State University	Ohio University
Case Western Reserve University	Loyola University of Chicago	The Pennsylvania State University
The University of Chicago	Marquette University	Purdue University
University of Cincinnati	The University of Michigan	Saint Louis University
Illinois Institute of Technology	Michigan State University	Southern Illinois University
University of Illinois	University of Minnesota	The University of Texas at Austin
Indiana University	University of Missouri	Washington University
The University of Iowa	Northwestern University	Wayne State University
Iowa State University	University of Notre Dame	The University of Wisconsin-Madison

—NOTICE—

This report was prepared as an account of work sponsored by an agency of the United States Government. Neither the United States Government nor any agency thereof, nor any of their employees, makes any warranty, express or implied, or assumes any legal liability or responsibility for the accuracy, completeness, or usefulness of any information, apparatus, product, or process disclosed, or represents that its use would not infringe privately owned rights. Reference herein to any specific commercial product, process, or service by trade name, trademark, manufacturer, or otherwise, does not necessarily constitute or imply its endorsement, recommendation, or favoring by the United States Government or any agency thereof. The views and opinions of authors expressed herein do not necessarily state or reflect those of the United States Government or any agency thereof.

Printed in the United States of America
Available from
National Technical Information Service
U. S. Department of Commerce
5285 Port Royal Road
Springfield, VA 22161

NTIS price codes
Printed copy: A06
Microfiche copy: A01

Distribution Category:
Environmental Control Technology
and Earth Sciences (UC-11)

ANL/ES-118

ARGONNE NATIONAL LABORATORY
9700 South Cass Avenue
Argonne, Illinois 60439

ANALYSIS OF THE GAMMA SPECTRA OF THE URANIUM,
ACTINIUM, AND THORIUM DECAY SERIES

by

Michael H. Momeni

Division of Environmental Impact Studies

September 1981

FOREWORD

This report is a summary of a program to develop an integrated gamma-ray spectroscopy system for use in measurement of concentrations of radionuclides in solid samples collected near active and inactive uranium mining, milling, and fuel-processing facilities. Use of high-resolution gamma detectors allows specific quantification of the level of ground contamination. A gamma spectra of a sample of uranium mill tailings may show more than 150 individual peaks between a 40- to 1500-keV energy band. This necessitated a meticulous calibration of the system for gamma energy, efficiency, and precise knowledge of intrinsic radionuclide intensities.

This work was initially sponsored by the Division of Safeguards, Fuel Cycle and Environmental Research, U.S. Nuclear Regulatory Commission, and was completed under auspices of the U.S. Department of Energy in support of the Uranium Mill Tailings Remedial Action Program.

concerning the impacts we observed at wetlands in the Yucatan and
whether their degradation is due primarily to overgrazing or to other anthropogenic
activities. We also discuss whether our findings in Peténiles reflect those of
other degraded tropical wetlands and whether they can be generalized to other
regions. Finally, we consider the implications of our results for management of
wetlands in the Yucatan and for the development of a sustainable
management response for wetlands.

This paper is organized as follows. In the next section we describe the
study area and methods used to collect data. In the third section we present the
results of our analyses of potential impacts on wetlands in Peténiles.

CONTENTS

	<u>Page</u>
FOREWORD	1
CONTENTS	5
FIGURES	6
TABLES	7
ABSTRACT	8
1. INTRODUCTION	8
2. SPECTROMETER SYSTEM	9
3. ANALYSIS OF GAMMA SPECTRA	15
3.1 Gamma Spectra	15
3.2 Shape Functions	19
3.3 Peak Search Routine	21
3.4 Deconvolution of a Gamma Spectrum	24
3.5 Determination of Radioactivity	25
3.5.1 Isotope Identification	28
3.5.2 Detection Limit	29
3.6 Calibration	29
3.6.1 Energy Calibration	29
3.6.2 Efficiency Calibration	34
4. GAMMA SPECTRA OF THE URANIUM, ACTINIUM, AND THORIUM DECAY SERIES	36
4.1 Gamma Energies and Quantum Yields	36
4.2 Conclusion	38
REFERENCES	74
APPENDIX A. PREPARATION AND ANALYSIS OF STANDARDS	77
APPENDIX B. POLYNOMIAL COEFFICIENTS FOR THE EFFICIENCY FUNCTION AND STATISTICS OF LEAST-SQUARES FIT OF DATA	99
ACKNOWLEDGMENTS	100
DISTRIBUTION LIST	101

FIGURES

<u>Figure</u>	<u>Page</u>
1.1 Uranium-238 Decay Series	10
1.2 Thorium Decay Series	11
1.3 Actinium Decay Series	12
 2.1 Diagram of the Gamma Spectrometer	14
 3.1 Gamma Spectra of Natural Uranium Sample, 0-1400 keV	16
3.2 Gamma Spectra of Natural Thorium Sample, 0-1400 keV	17
3.3 Gamma Spectra of Uranium and Thorium Ores, 40-70 keV	18
3.4 Gamma Spectra of Uranium and Thorium Ores, 70-120 keV	18
3.5 Peak Shape Parameters for a Gaussian Peak Folded into a Step Function and an Exponential Function, $r = (x-x_j)/\rho_j$	22
3.6 Flow Diagram of the Spectral Analysis Program	23
3.7 Decay of ^{238}U to ^{234}Th and ^{234}Pa	26
3.8 Flow Diagram of the Program for Isotope Detection and Calculation of Radioactivity	30
3.9 Energy Calibration of Gamma Spectra, 0-200 keV	32
3.10 Calculated Energy Minus Observed Energy (residuals) of Gamma Spectral Energy Calibration for Region 1	33
3.11 Energy Calibration of Gamma Spectra, 200-1400 keV	33
3.12 Calculated Energy Minus Observed Energy (residuals) of Gamma Spectral Energy Calibration of Region 2	34
3.13 Calculated Efficiency and Measured Efficiency as a Function of Photon Energy	35
 4.1 Gamma Spectra of the Uranium and Thorium Ores, 40-70 keV	69
4.2 Gamma Spectra of the Uranium and Thorium Ores, 70-120 keV	69
4.3 Gamma Spectra of the Uranium and Thorium Ores, 120-200 keV	70
4.4 Gamma Spectra of the Uranium and Thorium Ores, 200-400 keV	70
4.5 Gamma Spectra of the Uranium and Thorium Ores, 400-600 keV	71
4.6 Gamma Spectra of the Uranium and Thorium Ores, 600-800 keV	71
4.7 Gamma Spectra of the Uranium and Thorium Ores, 800-1000 keV	72
4.8 Gamma Spectra of the Uranium and Thorium Ores, 1000-1200 keV	72
4.9 Gamma Spectra of the Uranium and Thorium Ores, 1200-1400 keV	73

TABLES

<u>Table</u>	<u>Page</u>
2.1 Average Background Count Rates at Selected Energies	15
3.1 Energy Calibration	31
4.1 Detected Peaks in a Sample of Ore Containing Uranium and Actinium Series in Secular Radioactive Equilibrium	40
4.2 Detected Peaks in a Sample of Ore Containing Uranium, Actinium, and Thorium Series in Secular Radioactive Equilibrium	45
4.3 Energy and Quantum Yield of Selected Nuclides in the Uranium Series	49
4.4 Energy and Quantum Yield of Selected Nuclides in the Actinium Series	51
4.5 Energy and Quantum Yield of Selected Nuclides in the Thorium-232 Series	52
4.6 Energy and Quantum Yield of Nuclides in the Uranium Series: Comparison of Values Measured in This Study with Those Previously Reported	53
4.7 Energy and Quantum Yield of Nuclides in the Actinium Series: Comparison of Values Measured in This Study with Those Previously Reported	59
4.8 Energy and Quantum Yield of Nuclides in the Thorium Series: Comparison of Values Measured in This Study with Those Previously Reported	63

ANALYSIS OF THE GAMMA SPECTRA OF THE URANIUM,
ACTINIUM, AND THORIUM DECAY SERIES

by

Michael H. Momeni

ABSTRACT

This report describes the identification of radionuclides in the uranium, actinium, and thorium series by analysis of gamma spectra in the energy range of 40-1400 keV. Energies and absolute efficiencies for each gamma line were measured by means of a high-resolution germanium detector and compared with those in the literature. A gamma spectroscopy method, which utilizes an on-line computer for deconvolution of spectra, search and identification of each line, and estimation of activity for each radionuclide, was used to analyze soil and uranium tailings, and ore.

1. INTRODUCTION

Gamma-ray spectroscopy provides an inexpensive and efficient method for measuring the contamination of the environments of facilities processing natural, depleted, and enriched uranium. In general, radionuclide concentrations in environmental samples may be determined by means of radiochemical separations, followed by alpha- and beta-ray spectroscopy. But these techniques, in comparison with high-resolution gamma-ray spectroscopy, are laborious and time consuming, preventing an extensive sampling procedure often demanded by environmental programs. In recent years, the application of on-line minicomputers to the analysis of complex gamma-ray spectra has further

facilitated and tailored the process of data reduction, error analysis, and search for radionuclides in the uranium, thorium, and actinium decay series.

Figures 1.1 through 1.3 depict the decay series of uranium (U-238), thorium (Th-232), and actinium (U-235). The structures and emission characteristics of these series have been studied by Hyde, Perlman and Seaborg (1964); Lederer, Hollander and Perlman (1968); Gunnink et al. (1969); Kogan et al. (1969); Adams and Gasparini (1970); Smith and Wollenberg (1972); Davidson and Conner (1968); Lingeman et al. (1969); Bjornholm et al. (1968); and Godart and Gizon (1973). The most recent compilation of gamma-ray spectra recorded by germanium detectors is that of Heath (1975). However, in many cases, the reported intensities do not agree, and the absolute intensities are not available.

High-resolution germanium detectors are capable of recording more than 150 distinct peaks within the 40 keV to 2 MeV energy region. Deconvolution of gamma-ray spectra, identification of radionuclides from the gamma lines, and calculation of the concentration of each radionuclide demand accurate knowledge of both gamma energies and the intensities of the gamma transitions of each radionuclide. In this report, procedures for deconvolution of gamma-ray spectra and radionuclide identification are described. Gamma transition intensities and energies for the prominent peaks were measured and compared with those reported in the literature.

2. SPECTROMETER SYSTEM

The application of a gamma spectrometer to measurements of environmental samples requires the following:

1. A resolution better than 2 keV [full-width-half-maximum (FWHM)] at the 1.33 MeV peak of Co-60,
2. A lower detection limit of 40 keV and an upper limit of 2 MeV,
3. Relative photopeak efficiency of more than 10%,
4. Low background,

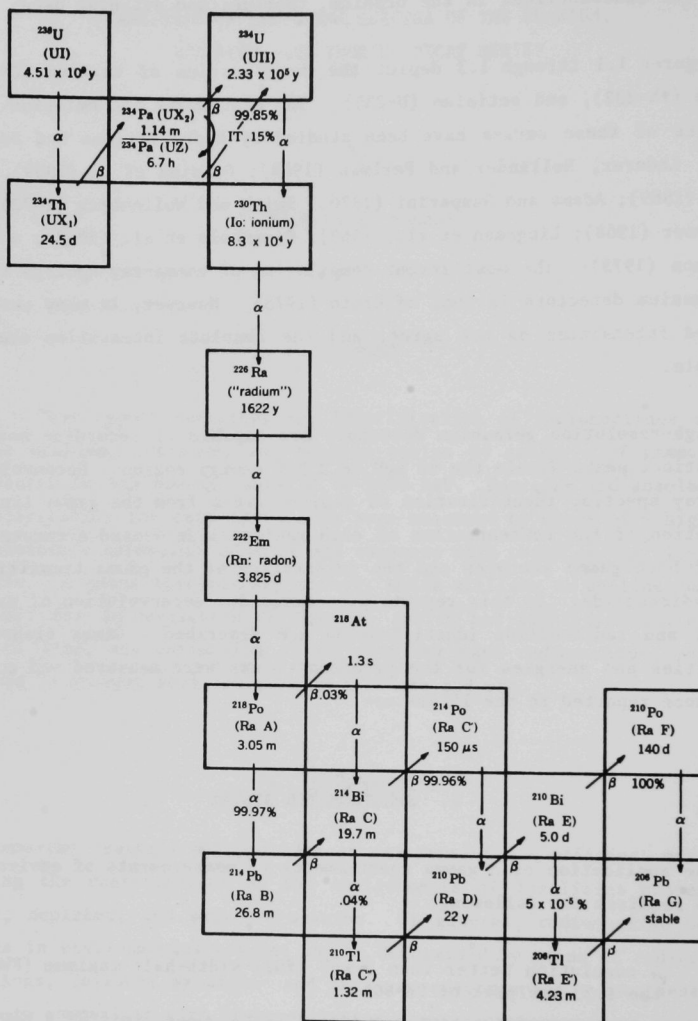


Figure 1.1. Uranium-238 Decay Series.

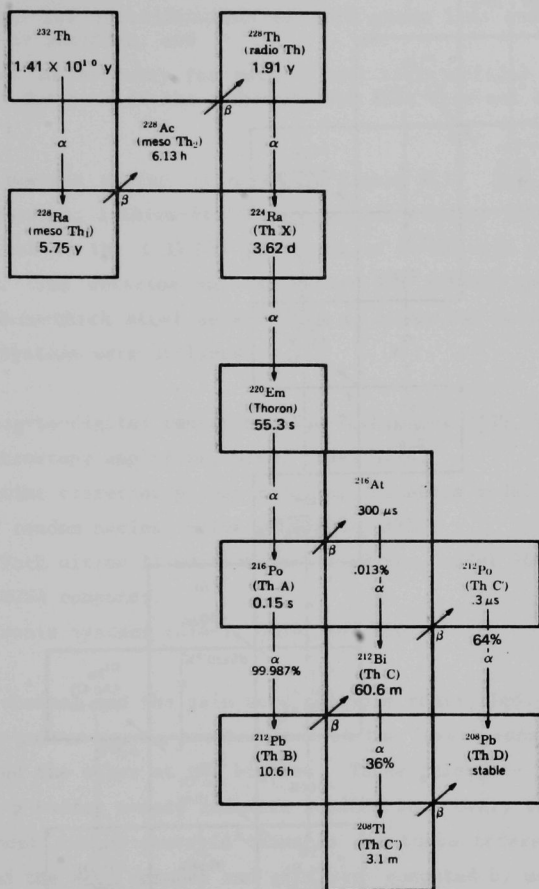


Figure 1.2. Thorium Decay Series.

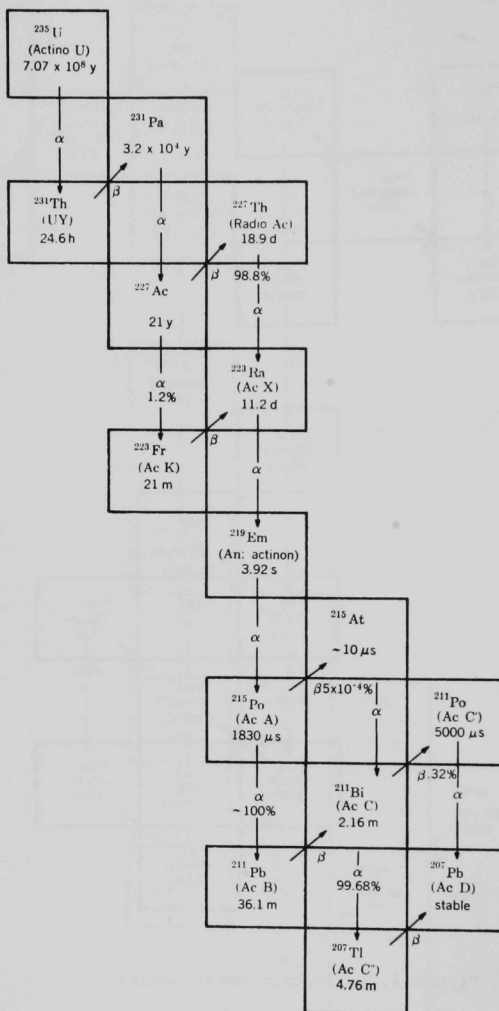


Figure 1.3. Actinium Decay Series.

5. Stable electronics suitable for long-duration measurements of low-activity samples,
6. A software package for deconvolution of complex gamma spectra,
7. A procedure for identification of each gamma line and assignment to a nuclide or nuclides, and
8. Calculation of activity for each of the radionuclides and the detection limit for each of the radionuclides that were not observed.

The spectrometer design is shown in Figure 2.1. The detector is an upward, true coaxial, lithium-drifted germanium detector (ORTEC) with a resolution of 1.8 keV at the 1.33 MeV photopeak of Co-60 with a peak to Compton ratio of 44:1. The detector and the cooled FET (ORTEC) preamplifier are housed in a 12-cm-thick steel shield that is about 100 cm above the ground. The following systems were utilized:

1. Analog-to-digital converter, Ino-Tech model 2105, 50 MHz.
2. Spectroscopy amplifier, Ortec Model 472A.
3. Livetime corrector/pileup rejector, Canberra model 1468.
4. Dual random nuclear pulse generator, ANL.
5. Ino-Tech ultima II multichannel analyzer, model 3408.
6. 32k NOVA computer.
7. Tektronix systems 4014-1, 4054, and 4907.

The zero channel and the gain were software controlled. Two energy-stable, random nuclear pulses were generated, one at the lowest energy channel (first 10 channels) and the other at the highest. These reference pulses (10,000 cps) were stored in a buffer memory and were scanned once every 100 seconds. Subsequently, the most likely centroid channels for these reference pulses were calculated, and the zero channel and gain were computed by means of these centroids. The sample spectrum collected within the next 100 seconds was then adjusted for the channel location. Comparison of the centroids calculated over a period of time for a gamma line of known intensity, within an energy range of 40 keV to 2 MeV, showed no evidence of drift in gain or degradation of peak resolution. Table 2.1 shows the background count rates at selected gamma energies measured for periods of 70 hours, as well as the estimated errors of deconvolution of the gamma spectra.

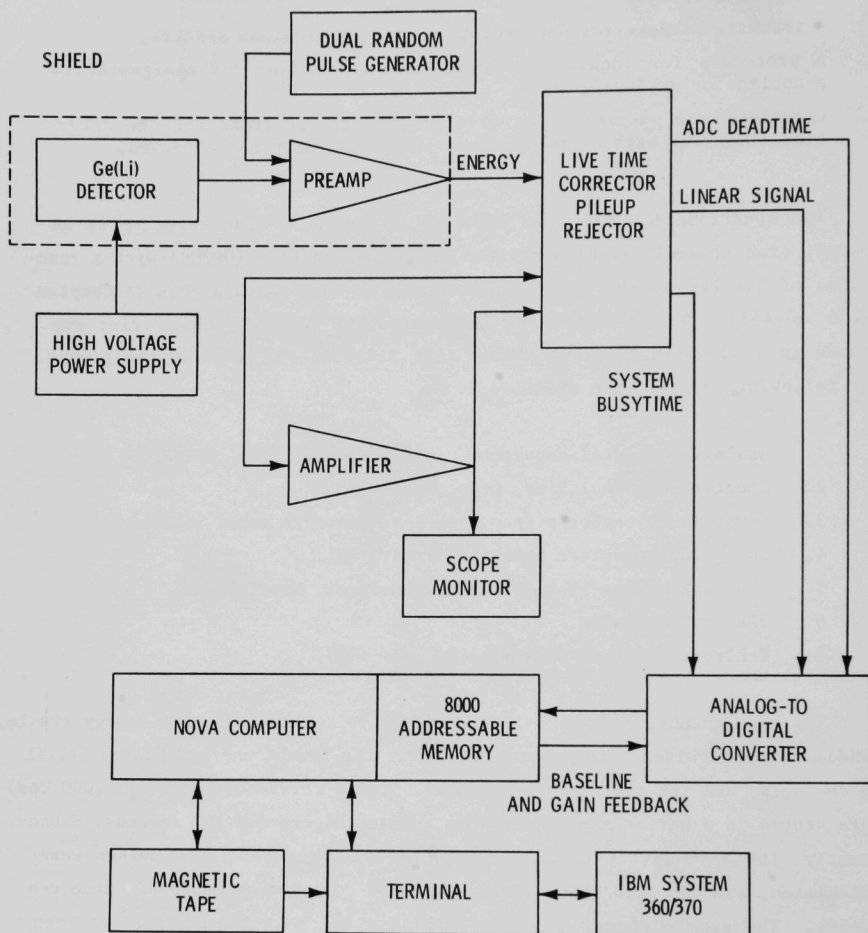


Figure 2.1. Diagram of the Gamma Spectrometer.

Table 2.1. Average Background Count Rates at Selected Energies

Energy (keV)	Area (counts)	Error (%) Area	Count Rate (cpm)	Radionuclide
46.5	250	28.90	5.95E-2	Pb-210
63.3	468	31.20	1.11E-1	Th-234
92.8	1395	8.85	3.32E-1	Th-234
185.7	997	11.85	2.37E-1	U-235/Ra-226
238.6	1368	7.50	3.26E-1	Pb-212
351.8	670	14.25	1.60E-1	Bi-211/Pb-214
510.7	5692	7.95	1.36E 0	Tl-208
609.4	378	11.95	9.06E-2	Bi-214
727.3	100	34.0	2.38E-2	Bi-212/Ac-228
911.1	306	12.25	7.29E-2	Ac-228
988.1	179	13.90	4.26E-2	Ac-228
1238.2	52	26.0	1.24E-2	Bi-214

3. ANALYSIS OF GAMMA SPECTRA

3.1 Gamma Spectra

The gamma spectra of natural uranium and thorium samples in the 40- to 1400-keV range are shown in Figures. 3.1 and 3.2. Stripping the spectra for calculation of the area under each peak, e.g., at 46.5 keV of Pb-210 (Fig. 3.3), requires correction for the contribution of the adjacent peaks and the continuum. The shape of each observed peak is not truly Gaussian; it rises sharply on the high energy side and skews on the low energy side (response function). The ideal distribution of a gamma-ray with a negligible natural energy width is Gaussian, but because of equipment noise, incomplete charge collection, pileup, and escape of annihilation radiation, the distribution at the low-energy side is exponential. Thus, a discontinuity appears in the background continuum above and below the initial gamma photopeak. Moreover, on occasion, neighboring peaks will overlap, precluding any simple hand calculation or electronic integration of the area above the continuum, e.g., the regions between 70-80 keV (Fig. 3.4).

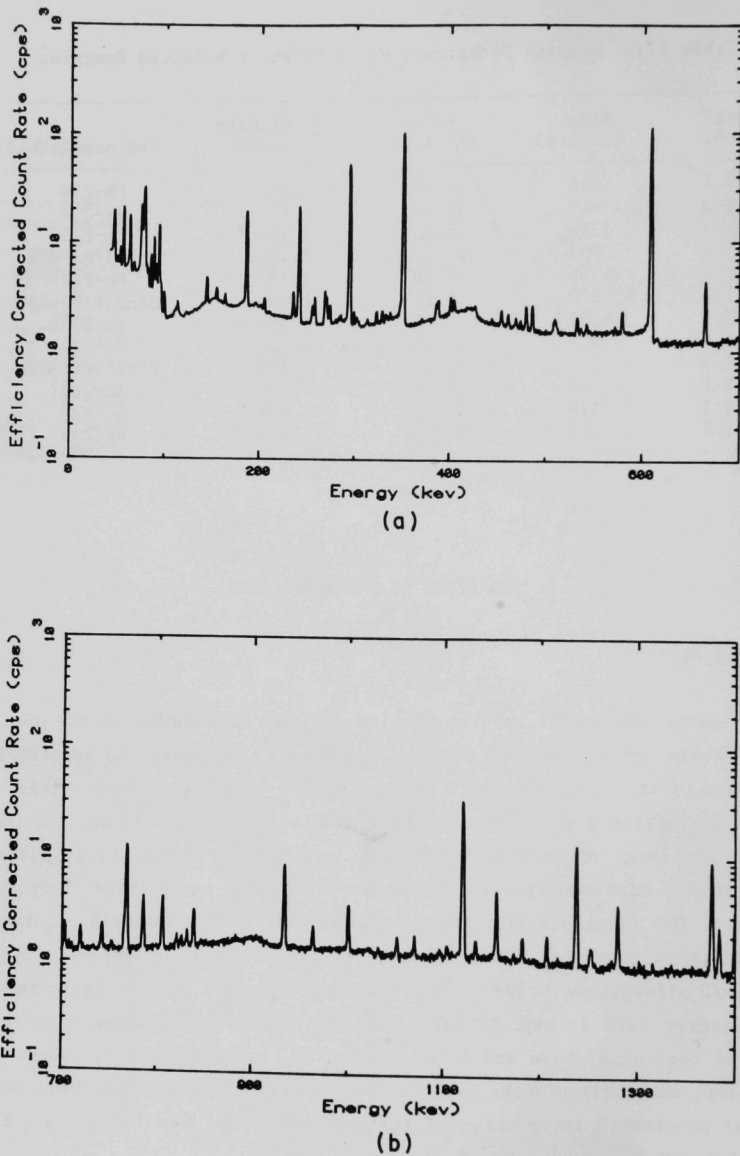


Figure 3.1. Gamma Spectra of Natural Uranium Sample, 0 - 1400 keV.

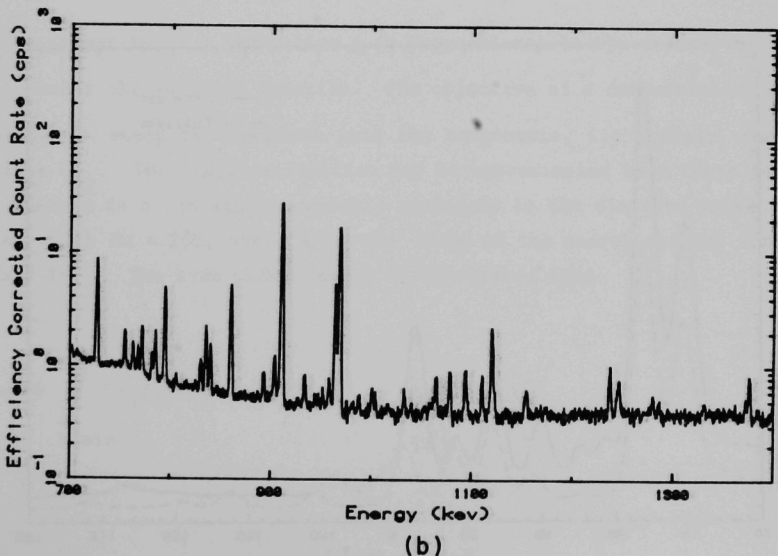
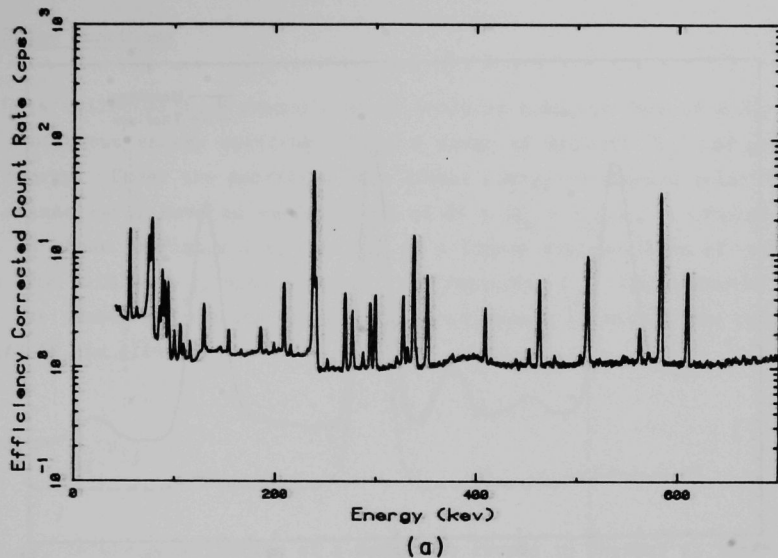


Figure 3.2. Gamma Spectra of Natural Thorium Sample, 0 - 1400 keV.

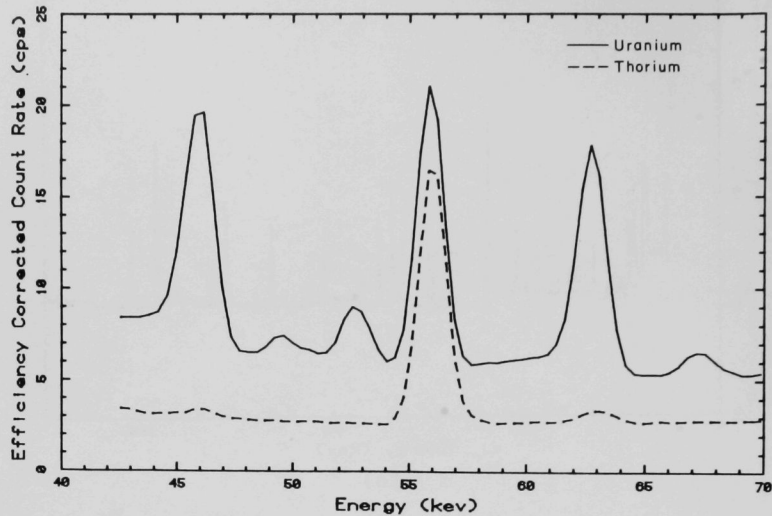


Figure 3.3. Gamma Spectra of Uranium and Thorium Ores, 40 - 70 keV.

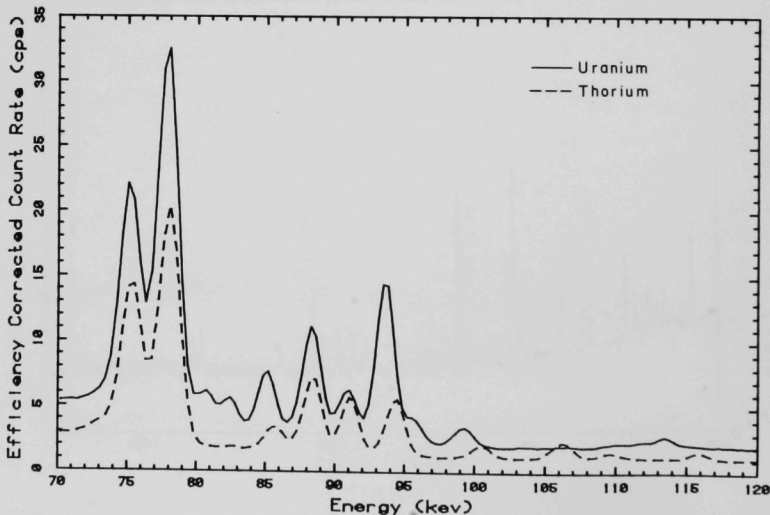


Figure 3.4. Gamma Spectra of Uranium and Thorium Ores, 70 - 120 keV.

3.2 Shape Functions

Data collected in N channels of an analyzer take the form of a histogram of a continuous energy spectrum within a range of minimum (E_o) and maximum (E_m) energy. Under the condition of a linear energy-to-channel relationship, each channel will have an energy width of $\delta E = (E_m - E_o)/N$. A complex spectrum, as shown in Figure 3.1, consists of a linear superposition of contributions from each peak j , with energy E_j and intensity a_j . The number of counts, i.e., the number of photons detected with an energy E , within the range of $E \pm 1/2 \delta E$, is given by

$$n_i = \sum_{j=1}^k n_{ij} ,$$

where n_{ij} is the contribution of a peak j to counts in channel i . The summation extends over the entire gamma spectrum, even though, on occasion, the upper energy E_k could exceed E_m .

The intensity of a gamma line j is proportional to the area $a_j = \sum_{i=1}^n n_{ij}$ under the response function. The objective of a deconvolution procedure is to strip the spectrum into the components, i.e., peaks, and to calculate n_{ij} . The response function may be approximated by a shape function $f(x)$, where x is a continuous variable analogous to the discrete index i and a channel width $\delta x = K\delta E$, where K is the slope of the energy channel function ($dE/dx = K^{-1}$). The area under peak j is calculated from

$$a_j = \int_{x \text{ min}}^{x \text{ max}} f_j(x) dx .$$

An individual peak, a_j , is superimposed on a continuum, which, within the region of integration, may be represented by a polynomial

$$f_c(x) = A_0 + A_1 (x - x_j) + A_2 (x - x_j)^2 ,$$

where x_j is the centroid to the peak j , the region of interest, and A_j is the amplitude of peak j . The shape function $f_p(x)$ for each peak j is a Gaussian function $f_g(x)$, where

$$f_g(x) = A_j \exp \left[-\left(\frac{(x - x_j)}{\rho_j} \right)^2 \right] ,$$

folded into an exponential function. The parameters of function $f_g(x)$ are as follows:

A_j = the peak amplitude.

x = the channel location.

x_j = the centroid for peak j of energy E_j .

ρ_j = the peak width (FWHM)/2.

The addition of an exponential function to the low-energy side of peak j and the change of the log base from "e" to "2" in the above equation results in

$$f_p(x) = A_j 2^{[-(x-x_j)^2/\rho_j^2]} ,$$

when

$$-\alpha \leq [(x-x_j)/\rho_j] \leq \beta ;$$

$$f_p(x) = A_j 2^{[\alpha^2 + 2\alpha(x-x_j)/\rho_j]} ,$$

when

$$[(x-x_j)/\rho_j] < -\alpha ;$$

and

$$f_p(x) = A_j 2^{[\beta^2 - 2\beta(x-x_j)/\rho_j]} ,$$

when

$$(x-x_j) > \beta ;$$

where α is the skewing parameter for joining the Gaussian to the exponential function, and β is the upper energy cutoff channel. In addition, a step function, $f_s(x)$, is also included in the low-energy side of the peak (Fig. 3.5). The step function $f_s(x)$ for a relative step height δ is expressed as

$$f_s(x) = A_j \delta \left\{ 2^{-[1.75(x-x_j)/\rho_j]} \right\} ,$$

when

$$(x-x_j)/\rho_j \geq 0 ;$$

and as

$$f_s(x) = A_j \delta \left\{ 2^{-2[1.75(x-x_j)/\rho_j]} \right\} ,$$

when

$$(x-x_j)/\rho_j < 0 .$$

The computer program for this analysis was written for use on a NOVA computer. Figure 3.6 shows the program flow diagram.

3.3 Peak Search Routine

The initial procedures in deconvolution of a spectrum are separation of the true peak from statistical fluctuations and estimation of the contribution

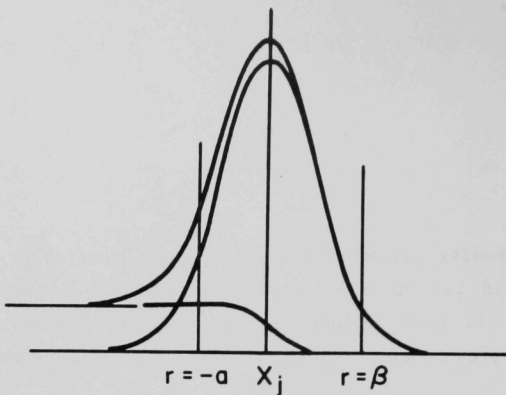


Figure 3.5. Peak Shape Parameters for a Gaussian Peak Folded into a Step Function and an Exponential Function,
 $r = (x-x_j)/\rho_j$.

to the continuum from other background features such as the Compton edge. In this program, the high frequency noise and the low frequency background are filtered by means of a square-wave correlator convolution function with a zero area (Philips and Marlow 1976). In the absence of a peak, the expected value of the correlator signal through the data is zero. In the presence of a peak, the expected value of the correlator signal in a channel "i" exceeds a pre-selected number (search sensitivity value) of standard deviations of the measured count in that channel. The choice of a square-wave correlator with a width of about the same magnitude as the true width of the peaks effectively eliminates detection of statistical fluctuations as true peaks. Detailed discussions of the parameters affecting the deconvolution process and of data reduction are given by Fletcher and Powell (1963); Davidson (1965); Kearn (1969); Brown and Dennis (1970); Beeck (1975); McNelles and Campbell (1975); Brassard and Correias (1977); and Momeni (1978).

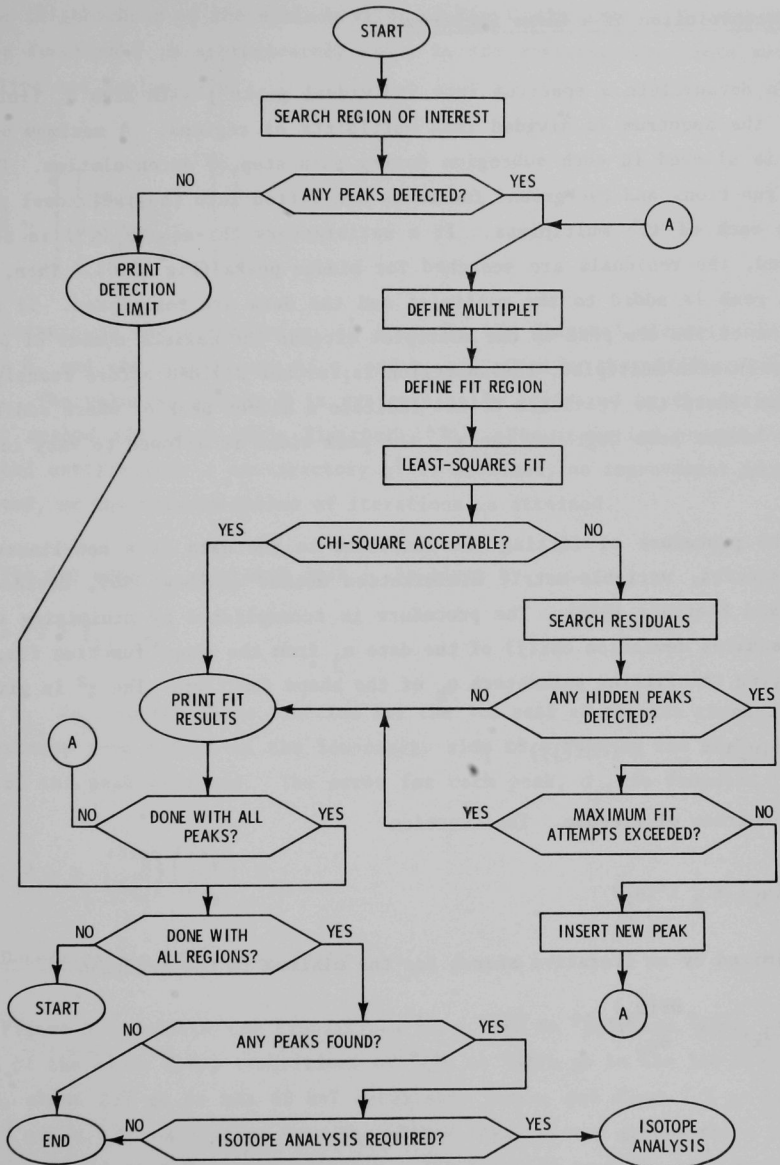


Figure 3.6. Flow Diagram of the Spectral Analysis Program.

3.4 Deconvolution of a Gamma Spectrum

To deconvolute a spectrum into individual peaks j with area a_j (intensity), the spectrum is divided into multiplets of regions. A maximum of 6 peaks is allowed in each subregion during each step of deconvolution. Peak shape functions and background functions are fitted into the individual peaks within each of the multiplets. If a satisfactory chi-square (χ^2) is not achieved, the residuals are searched for hidden peaks (Fig. 3.6). Then, the hidden peak is added to the multiplet and the data are reanalyzed. If the addition of the new peak to the multiplet exceeds the maximum number of peaks allowed in each multiplet, the subregion is further divided before reanalysis. In cases where the residuals do not indicate a hidden peak or where addition of the hidden peak degrades the χ^2 , the peak width is allowed to vary independently.

The procedure of fitting the functions to the data is a non-linear, least-squares, variable-metric minimization method (Garbow 1969, Davidson 1965, and Fletcher 1970). The procedure is accomplished by minimizing the least-squares deviation $\chi(j)$ of the data n_j from the shape function $f(x, q_k)$, by varying the fitting parameters q_k of the shape function. The χ^2 is given by

$$\chi^2(q_k) = \frac{1}{n_f} \sum_j (\chi(j))^2 ,$$

for n_f degrees of freedom. The function

$$F(q_k) = \frac{1}{2} \chi^2(q_k)$$

is optimized by an iterative search for the minimum in the function

$$G(q_k, i) = \frac{\partial F(q_k)}{\partial q_k} .$$

In the neighborhood of the minimum value of $F(q_k)$, the inverse Hessian matrix of the function F is approximately equal to the variance-covariance matrix (Phillips and Marlow 1976)

$$H \approx \left| \begin{array}{c} \\ \frac{\partial^2 F(q_{ik})}{\partial q_i \partial q_k} \\ \end{array} \right|^{-1} .$$

The variance in the parameter q_i is given by the diagonal elements of the matrix H , and the covariances of q_i and q_j are given by the off-diagonal elements. The value of matrix H is systematically estimated by the variable-metric method (Davidson 1965, Fletcher 1970). The iteration procedure is repeated until either a satisfactory χ^2 is obtained, no improvement in χ^2 is achieved, or the maximum number of iterations is attained.

The net area a_j , for each peak j , is given by

$$a_j = \sum_i f_{ij}(q_k) ,$$

where $f_{ij}(q_k)$ is the shape function for the j th peak at the i th channel. The sum extends from 8 FWHM on the low-energy side to 4 FWHM on the high-energy side of the peak centroid. The error for each peak, σ_j , is computed from

$$\sigma_j^2 = \sum_{ik} \left(\frac{\partial a_k}{\partial q_i} \right) \left(\frac{\partial a_k}{\partial q_k} \right) H_{ik} .$$

3.5 Determination of Radioactivity

Figure 3.7 depicts the transitions from $^{238}_{92}\text{U}$ to $^{234}_{90}\text{Th}$ and $^{234}_{91}\text{Pa}$. About 0.23% of the alpha decay transitions of $^{238}_{92}\text{U}$ to $^{234}_{90}\text{Th}$ go to the 160 keV excited state, about 23% go to the 50 keV metastable state, and about 77% go to the ground state. De-excitation from the 50-keV level to the ground state results in emission of 50-keV gamma radiation. $^{234}_{90}\text{Th}$ decays to $^{234}_{90}\text{Pa}$ by β emission. About 72% of the beta transitions from the ground state of $^{234}_{90}\text{Pa}$ to the excited

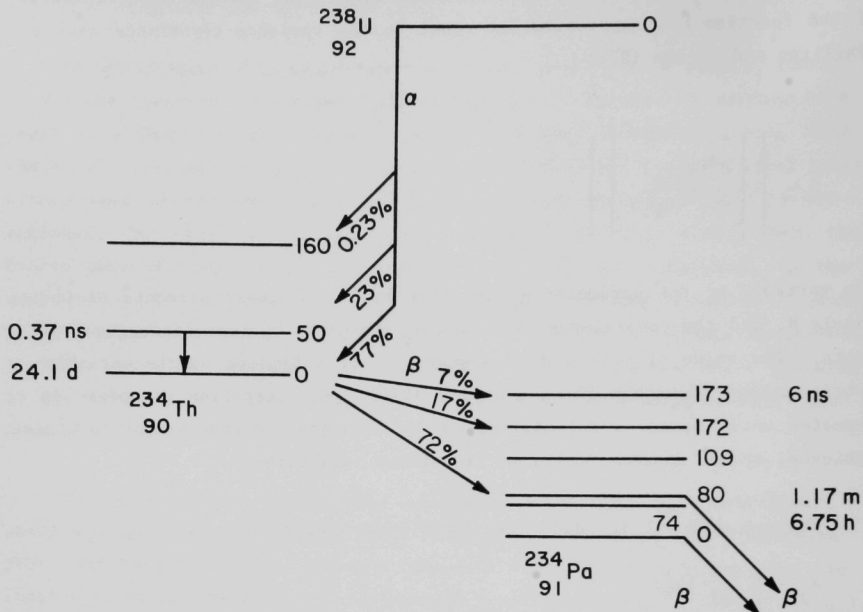


Figure 3.7. Decay of ^{238}U to ^{234}Th and ^{234}Pa .

state of Pa-234 go to the 1.17-minute metastable state of ~ 80 keV, 17% to the 172.9-keV level; and 7% to the 173.3-keV level. Only 0.13% of the transitions from the 1.17 minute metastable state to the ground state of ^{234}Pa are internal; the remainder are β decays to the U-234 nuclide. De-excitation from the excited states of ^{234}Pa to the ground state occurs by gamma emission. Transitions of the other nuclides in the uranium, actinium, and thorium series are reported by Lederer, Hollander and Perlman (1968) and in recent revision in (1978).

Gamma emissions from the decay of any of the nuclides in any of the series exhibit a set of discrete lines that can be used for the identification

of the nuclide. Associated with each set of gamma lines is a set of intensities corresponding to the areas of the peaks a_j . The number, N , of decays of a radionuclide p from a sample with an activity A_p (in pCi) is

$$N_p = 2.22 A_p .$$

Of these transitions, a fraction b_{pj} are photons with energy E_j given by

$$N_{pj} = b_{pj} N_p .$$

Thus, corresponding to a set of photons with energies E_j are intensities b_{pj} , which are detected at the peak locations j . The fraction of the photons with the energy E_j detected at j is dependent on the detector size, sample configuration, detection geometry and the sample matrix. This fraction, n , is a function of energy and is given by

$$n_{pj} = \varepsilon_j N_{pj} ,$$

where ε_j is the total detection efficiency of the gamma spectrometer system. Therefore, the activity A_{pj} (in pCi) is calculated from

$$A_{pj} = \frac{n_{pj}}{2.22 b_{pj} \varepsilon_j} .$$

The average activity $\langle A_p \rangle$, estimated from all gamma lines emitted by the radionuclide p , is given by

$$\langle A_p \rangle = \frac{\sum_j w_j A_{pj}}{\sum_j w_j} ,$$

where the summation is over all gamma lines emitted during transition of a radionuclide p to its immediate daughter. The weight factor W_{pj} is given by

$$W_{pj} = \left(\frac{1}{\sigma_a^2_{pj}} \right)^2 = \left(\frac{\epsilon_j b_{pj}}{\sigma_a^2_{pj}} \right)^2 ,$$

where $\sigma_a^2_{pj}$ is the error from the estimation of the area of peak j . The statistical error associated with the average activity is the standard propagated statistical error:

$$\sigma^2_{\langle A_p \rangle} = \frac{\sum W_{pj}^2 \sigma_a^2_{pj}}{(\sum W_{pj})^2} .$$

In addition, the chi-square error from the deconvolution procedures is estimated from the minimum variance error by

$$\sigma^2_{\text{chi-square}} = \frac{\sum W_{pj} (a_{pj} - \langle A_p \rangle)^2}{(N-1) \sum W_{pj}}$$

under the condition that when $N = 1$, $\sigma^2_{\text{chi-square}} = 0$, where N is the number of counts.

3.5.1 Isotope Identification

A set of gamma lines j with distinct intensities b_{pj} unambiguously identifies the presence of isotope p . The intensity of these lines can vary significantly from very faint to intense. Detection of the faint lines requires long acquisition time and occasionally may be unsuccessful during the peak search analysis. For example, a sample with an activity of 1 pCi of an isotope p and a photon intensity of $b_{pj} = 1 \times 10^{-2}$ emits only 2.22×10^{-2} photons/min. At a detection efficiency of 15%, only 3.33×10^{-3} gammas of energy E_j are detected each minute, or 4.8 each day. This count rate is significantly smaller than the statistical fluctuation in the spectrometer background. Thus, for a sample with such low activity, the gamma line will not be

perceptible. Therefore, the procedure for identification of an isotope on the basis of presence of all lines can fail even though the major lines are present. In our study, the procedure for identification of an isotope is based on the presence of the major lines, which are selected on the basis of their relative intensities. Figure 3.8 depicts the flow diagram of the program for isotope detection and activity calculation. Nuclides are identified by comparing the subset of the gamma lines (major lines) detected in the spectrum with those in the isotope library.

3.5.2 Detection Limit

The analysis of a sample often entails the calculation of the lowest detectable activity as an upper bound estimate of the concentration of a radionuclide not detected during the measurement. The algorithm for this calculation is based on the minimum peak detection correlator signal at the most prominent photon peak of the isotope. The net peak area a_d associated with this line is computed for a peak with a mean correlator signal that is two standard deviations above the minimum detection signal and that assumes a Gaussian shape with a width (FWHM) adopted from the calibration procedure. Therefore, the minimum detectable activity is calculated from

$$A_p = a_d / (2.22 \varepsilon_j b_{pj}) .$$

3.6 Calibration

3.6.1 Energy Calibration

The purpose of energy calibration is to determine the functional relationship between energy and channel number. The initial step is determination of channel number and energy of a set of precisely known gamma lines. The preparation and analyses of the standards are described in Appendix A. The standards used for energy and efficiency calibration were the following:

- a. Radium (Ra-226) in secular radioactive equilibrium (National Bureau of Standards reference material 4959-130) with an uncertainty of 1.2% in the specified activity.

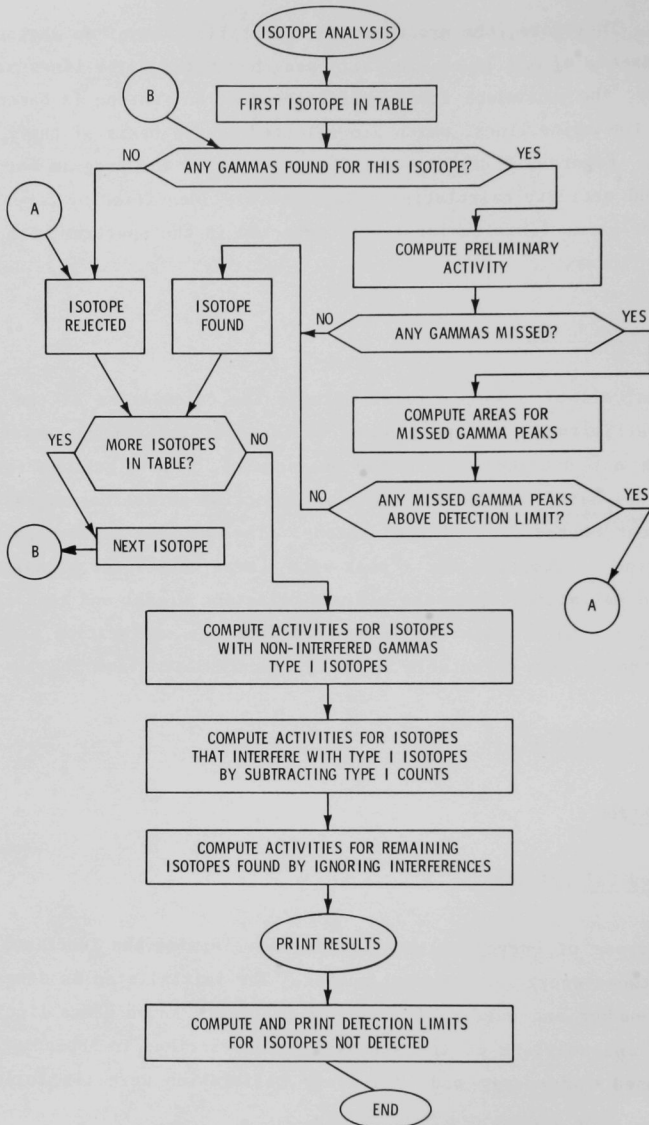


Figure 3.8. Flow Diagram of the Program for Isotope Detection and Calculation of Radioactivity.

- b. Mixed radionuclide, gamma-ray emission-rate solution (standard reference material 4243G) containing the following radionuclides (uncertainties in specified activity in parentheses): Cd-109 (3.1%), Co-37 (2.7%), Ce-139 (1.3%), Hg-203 (2.3%), Sn-113 (3.1%), Sr-85 (2.5%), Cs-137 (2.3%), Y-88 (3.1%), Y-88 (2.5%), and Co-60 (1.6%).
- c. Thorium ore ($1.01 \pm 0.01\%$) at a 95% confidence level, plus 0.04% uranium from New Brunswick Laboratory, Sample No. 79 (monozite sand, Th = 8.44%, in dunite).
- d. Pitchblende ore (53.55% U_3O_8), Sample No. 6, New Brunswick Laboratory.
- e. Additional gamma standards for energy were Am-241, Pb-210, and Se-75.

For a functional representation, the spectrum was subdivided into two regions, channels 1-400 and channels 401-4000. Then for each region, a polynomial function was fitted to the data (j, E_j) by a least-squares method. Table 3.1 gives the calibration coefficients A_j for the polynomial

$$E (\text{keV}) = A_0 + A_1 C + A_2 C^2 + A_3 C^3 + A_4 C^4 ,$$

where C is the channel number, with a digital offset of 40 channels.

Table 3.1. Energy Calibration

Coefficient	Region 1	Region 2
	Channels 1-400	Channels 401-4000
A_0	2.040168E+1	2.391331E+1
A_1	3.555993E-1	3.477040E-1
A_2	1.945887E-4	-1.763261E-6
A_3	-8.920941E-7	2.418152E-10
A_4	1.007525E-9	0

Figure 3.9 shows the data (j , E_j) superimposed on the calculated calibration curve for the region of channels 1-400 (#1). Figure 3.10 shows the residuals, i.e., calculated energy minus observed energy, for region #1. The maximum difference of 0.15 keV between the observed and the calculated energies may be partially due to the error in centroid location and the energy assignment. Similarly, the calibration curve for region #2 (channels 401-4000) is shown in Figure 3.11 and the residuals in Figure 3.12. In region #2, the maximum residual error is 0.17 keV.

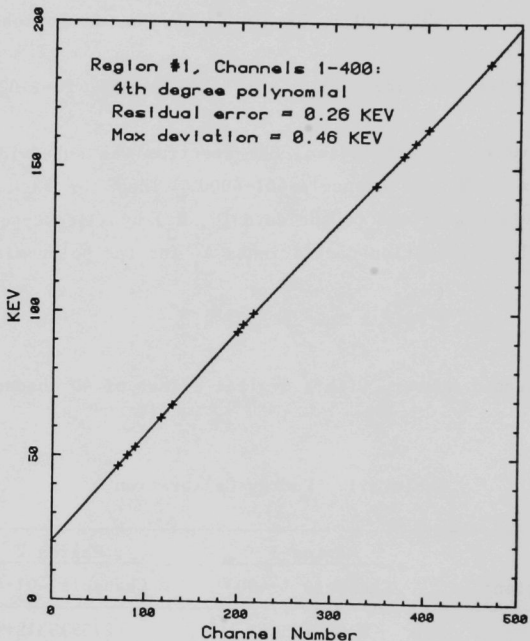


Figure 3.9. Energy Calibration of Gamma Spectra, 0 - 200 keV.

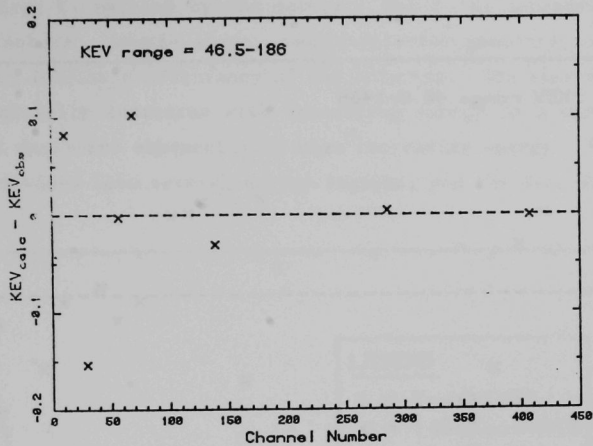


Figure 3.10. Calculated Energy Minus Observed Energy (residuals) of Gamma Spectral Energy Calibration for Region 1.

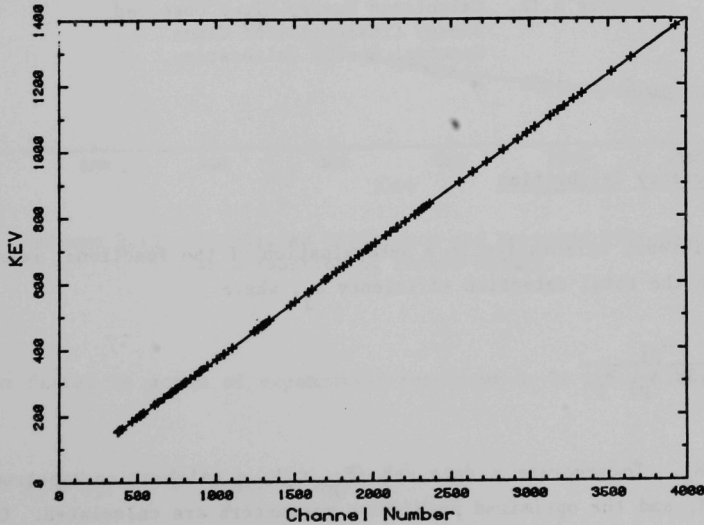


Figure 3.11. Energy Calibration of Gamma Spectra, 200 - 1400 keV.

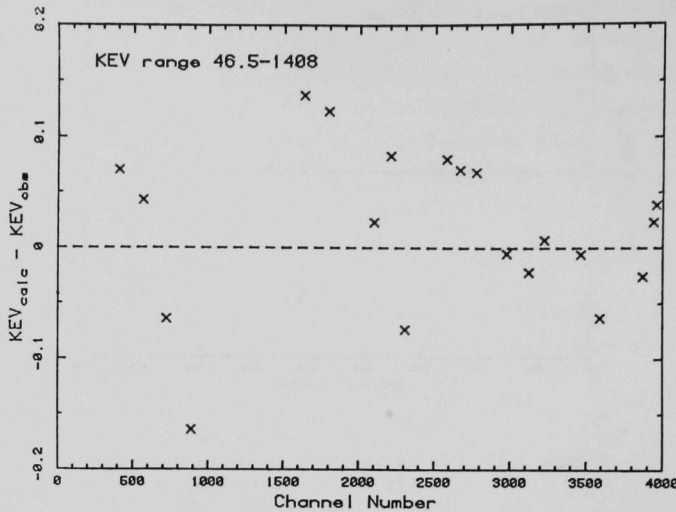


Figure 3.12. Calculated Energy Minus Observed Energy (residuals) of Gamma Spectral Energy Calibration.

3.6.2 Efficiency Calibration

An efficiency calibration is a determination of the functional relationship between the total detection efficiency ε_j , where

$$\varepsilon_j = \frac{n_{pj}}{2.22 A_{pj} b_{pj}},$$

and energy E_j . To generate a data set (E_j, ε_j) , a calibration spectrum is deconvoluted, and the optimized peak shape parameters are calculated. On the basis of this analysis and a known set of data $(E_j, 2.22 A_{pj} b_{pj})$, E_j and ε_j are calculated. The total efficiency, ε_j , is the detected fraction of the

photons of energy E_j emitted by the source. The ε_j is dependent on a combination of factors: sample shape, sample-detector geometry, sample self-absorption, and intrinsic efficiency of the detector. The observed efficiency (Fig. 3.13) initially increases with increasing energy to a maximum value; thereafter, it decreases exponentially with increasing energy. The efficiency curve can be divided into several energy regions, and the data in each region

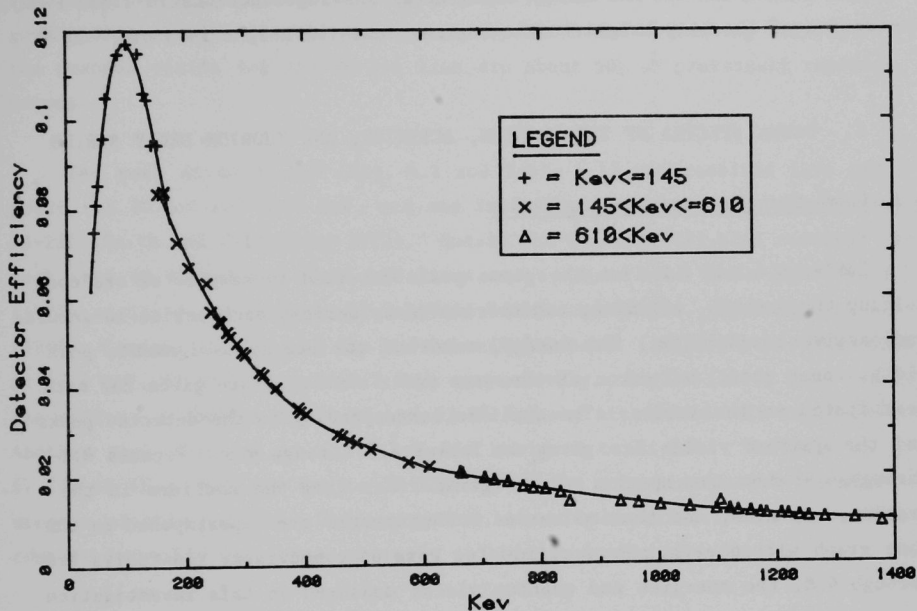


Figure 3.13. Calculated Efficiency and Measured Efficiency as a Function of Photon Energy.

are then fitted to a sum of exponential functions or to the following polynomial:

$$\varepsilon = A_0 + A_1 E + A_2 E^2 + A_3 E^3 + A_4 E^4 ,$$

calculated from a least-squares fit of the data (E_j , ε_j) to three energy regions: 40-145 keV, 145-610 keV, and 610-1500 keV. The coefficients A_i of

the polynomial are listed in Appendix B. The optimized peak width (FWHM) is a function of energy (E) and can be estimated by

$$\left(\frac{\text{FWHM}}{2}\right)^2 = R_0 + R_1 E ,$$

where $R_0 = 3.032$ and $R_1 = 3.69 \times 10^{-3}$. The peak shape parameter joining the central Gaussian to the low-energy exponential skewing functions is $1.833 \text{ FWHM}/2$. The ratio of the step height to the central Gaussian height is 3.018×10^{-2} .

4. GAMMA SPECTRA OF THE URANIUM, ACTINIUM, AND THORIUM DECAY SERIES

4.1 Gamma Energies and Quantum Yields

Tables 4.1 and 4.2 list the gamma peaks detected in samples of ore containing the uranium, actinium, and thorium decay series, each series in secular radioactive equilibrium. The energy, error of the energy assignment, peak width, count rate, and error of the area under each peak are given for each peak listed in the tables. The nuclides corresponding to the detected peaks and the quantum yields are given in Tables 4.3 through 4.5. Figures 4.1 through 4.9 show the spectra of the gamma lines from the nuclides in the uranium, actinium, and thorium series. The spectra are superimposed on the same graph within each energy region for ease of comparison. In Tables 4.6 through 4.8, the energies and quantum yields measured in this investigation are compared with those previously reported. Because the 70-115 keV region (Fig. 4.2) includes lines from X-ray emissions, the gamma line intensities were not estimated in this region, except for peaks at 92.75 keV (Th-234) and 109.15 keV (U-235) (see Tables 4.3 and 4.4).

The lowest energy peak detected in the spectrum of the uranium and actinium series (Table 4.1) is at 46.50 keV, and its origin is the decay of Pb-210. The quantum yield of this line is 4.10×10^{-2} , in good agreement with those previously reported (Table 4.6). In addition to this line, five other peaks are identifiable in Figure 4.1, and of these, three peaks also seem to be present in the thorium spectrum. The line at 57.62 keV is a reference line (pulse line) for comparison of the spectra. The thorium ore sample also contains uranium and actinium nuclides.

The second peak in the uranium spectrum was resolved into two peaks, 49.09 keV and 50.11 keV (Table 4.1), from Th-227, and Fr-223 at 49.8 keV also contributes to this peak (Table 4.4). The third peak was resolved into three peaks at 52.14, 52.77 and 53.18 keV (Table 4.1). The origin of the 52.77-keV line is uncertain. Smith and Wollenberg (1972) assigned the 52.14-keV line to Pb-214 and the 53.18-keV peak to U-234, but Lingeman et al. (1969) assigned the 53.23-keV peak to Pb-214. The quantum yields for the U-234 line are in good agreement with the values reported by Smith and Wollenberg (1972), but the quantum yields for the Pb-214 line are about 50% of previously reported values.

The peak at 63.42 keV (Fig. 4.1 and Table 4.1) was resolved into two peaks, 63.30 keV and 63.4 keV, and was assigned, respectively, to Th-234 and Pa-234 (Smith and Wollenberg 1972). Godard and Gizon (1973) also resolved the peak into 62.92 keV and 63.35 keV lines and assigned both to Th-234. Heath (1975) assigned the peak at 63.3 keV to Pa-231 and Th-234. Bjornholm et al. (1968), Sampson (1973), and Chu and Scharff-Goldhaber (1978) reported the peak at 63.4 keV, 63.28 keV, and 63.1 keV, respectively. Taylor (1973) also resolved the peak to a doublet at 62.97 and 63.35 keV and attributed both to Th-234. Another peak observed at 61.18 keV was assigned to Bi-214. The peak at 67.67 keV (Fig. 4.1) is due to Th-230 and is the only line useful for measurement of this nuclide. The energy and intensity reported in the literature compare favorably with those measured in this study (Table 4.6).

In the thorium series, the lowest energy detected (Table 4.2) was at 37.8 keV (not shown in Fig. 4.1). The origin of this line is uncertain. The next peak at 39.90 keV is from Bi-212 (Table 4.6). The other lines are from the uranium and actinium series. Because the 70-120 keV region includes lines from X-ray emissions (Fig. 4.2), the intensities for this region were not estimated except for the lines at 92.75 keV (Pa-234), 109.15 keV and 115.20 keV (U-235), and 113.08 keV (Th-227). The characteristic X-ray lines for elements contributing to the gamma spectra were previously reported (Lederer et al. 1968). The lines detected in the 70-120 keV energy region are listed in Tables 4.1 and 4.2. The prominent peaks in this energy region (Fig. 4.3) are at 143.82 keV (U-235, Th-230, Ra-223), 154.15 keV (Ra-223), 163.45 keV (U-235), and 185.93 keV (U-235, Ra-226) in the uranium and actinium series, and 129.07 keV (Ac-228) in the thorium series.

The lines from the nuclides in the uranium and actinium series, which were also observed in the thorium spectrum, are at 154.15 keV and 185.93 keV. The peak at 163.45 keV from the decay of U-235 has often been utilized for correction of the U-235 contribution to the unresolved lines (U-235 + Ra-226) at 185.93 keV for a direct measurement of Ra-226. For both lines, the energy and the quantum yield for U-235 are in good agreement with previously reported values (Table 4.7), but the quantum yield for Ra-226 is about 20% lower than those reported in the literature.

Tables 4.1 and 4.2 identify the most intense peaks observed in the spectra shown in Figures 4.3 through 4.5. The most suitable peaks for determination of activity are the intense peaks that are not complicated by interference. When the interference may be accounted for by other lines from the same nuclide, the peaks with interference can also be utilized for calculation of activities. However, in cases where the interference lines cannot be accounted for by other lines, the activities cannot be unambiguously determined. In some situations, the contribution from the interference lines is very weak, and the activity could be estimated, even though the magnitude of the interference is not computable.

The quantum yields measured in this investigation are generally of the same order of magnitude as those previously reported (Tables 4.6 through 4.8) but, in general, there is more favorable agreement for the more intense lines. The energies of the lines measured in this research are in good agreement with the previously reported values and within a fraction of a keV of the more recent measurements.

4.2 Conclusion

In general, the magnitude of the uncertainty associated with the computed quantum yield depends on the magnitude of the full width of the energy peak and the area under the peak, relative to the background continuum and the magnitude of the interferences. The uncertainty of estimating the contribution from the interference peaks is related to the magnitude of the uncertainty in the quantum yields and the uncertainty in the deconvolution method

for resolution of the multiplets. The uncertainty in the quantum yields of less than 1×10^{-3} is smaller than 5% for the lines free from interference and more than 10% for the others. The uncertainty arises from the composite errors of deconvolution, the uncertainty in the absolute activity of the primary standards, and the magnitude of the interference. This gamma spectroscopy system and the procedure for data reduction permit measurements of concentrations of the nuclides in uranium ore and tailings with total errors of less than 5%, and, for typical environmental concentrations, with total errors of less than 15%.

Table 4.1. Detected Peaks in a Sample of Ore Containing Uranium and Actinium Series in Secular Radioactive Equilibrium

Energy \pm Error (keV)	FWHM (keV)	Count Rate (cps)	Error (%)
46.50 \pm 0.01 ^a	1.14	5.480E-1	1.3
49.07 \pm 0.45 ^a	1.14	5.088E-2	4.45
50.11 \pm 0.14 ^a	1.14	5.088E-2	4.45
52.14 \pm 0.27 ^a	1.14	1.836E-1	2.20
53.18 \pm 0.04 ^a	1.14	1.836E-1	2.20
63.34 \pm 0.01 ^a	1.13	7.176E-1	0.75
67.67 \pm 0.05 ^a	1.13	7.490E-2	2.40
74.88 \pm 0.01 ^{a,b}	1.18	1.294E0	0.80
77.21 \pm 0.01 ^{a,b}	1.18	2.342E0	0.55
79.46 \pm 0.05 ^{a,b}	1.18	2.221E-1	3.35
81.30 \pm 0.05 ^{a,b}	1.18	1.842E-1	3.90
84.16 \pm 0.03	1.30	4.723E-1	8.40
87.65 \pm 0.01	1.27	7.375E-1	1.15
90.39 \pm 0.02 ^{a,b}	1.27	3.187E-1	1.15
93.23 \pm 0.01 ^{a,b}	1.27	1.125E0	0.60
95.38 \pm 0.03 ^{a,b}	1.27	1.400E-1	1.55
99.19 \pm 0.03 ^{a,b}	1.48	1.187E-1	3.10
103.52 \pm 0.19	1.45	7.937E-2	14.25
106.62 \pm 0.15 ^a	1.45	2.194E-3	84.70
110.07 \pm 0.10	1.45	1.655E-1	6.10
111.97 \pm 0.09	1.45	2.331E-1	4.75
113.86 \pm 0.04	1.45	5.385E-2	4.45
115.68 \pm 0.15	1.45	7.985E-2	11.05
123.75 \pm 0.33 ^a	1.14	1.354E-2	18.70
131.49 \pm 0.33	1.20	9.085E-3	17.55
139.87 \pm 0.30	1.25	1.189E-2	13.75
144.24 \pm 0.03	1.25	1.423E-1	1.85
154.25 \pm 0.06	1.35	5.655E-2	3.10
158.39 \pm 0.51	1.35	3.821E-2	18.70
163.45 \pm 0.06	1.29	5.035E-2	7.90
165.50 \pm 0.01	1.29	4.658E-3	32.35

Table 4.1 (cont'd)

Energy ± Error (keV)	FWHM (keV)	Count Rate (cps)	Error (%)
186.04 ± 0.01	1.29	1.031E00	0.35
188.72 ± 0.49	1.49	4.339E-2	25.55
195.85 ± 0.24 ^a	1.56	1.220E-2	15.53
202.04 ± 0.17	1.37	4.563E-2	12.30
205.27 ± 0.04	1.15	3.396E-2	7.50
210.45 ± 0.16	1.05	6.552E-3	14.70
235.90 ± 0.05	1.18	6.094E-2	2.40
241.92 ± 0.01	1.23	8.933E-1	0.30
253.73 ± 0.87	1.27	6.664E-3	50.60
256.18 ± 0.04	1.21	3.246E-2	4.45
258.44 ± 0.32	1.21	5.769E-2	3.15
259.09 ± 0.40	1.21	3.785E-3	32.10
269.41 ± 0.02	1.25	6.894E-2	1.60
271.20 ± 0.02	1.25	5.572E-2	1.60
273.53 ± 0.40	1.25	9.239E-3	13.45
274.75 ± 0.05	1.25	3.412E-2	4.35
281.09 ± 0.25	1.30	3.013E-2	12.30
283.63 ± 0.36	1.30	3.539E-3	27.90
286.12 ± 0.10	1.30	7.548E-3	14.80
295.16 ± 0.0	1.26	1.859E00	0.30
299.93 ± 0.13 ^a	1.26	1.437E-2	8.40
302.64 ± 0.30 ^a	1.43	6.816E-2	12.95
304.55 ± 0.40 ^a	1.43	5.125E-2	16.00
314.34 ± 0.25	1.14	1.3930E-2	14.35
323.84 ± 0.06	1.24	1.540E-2	6.75
329.80 ± 0.07	1.44	1.219E-2	8.30
333.97 ± 0.19 ^a	1.44	6.511E-2	8.20
338.29 ± 0.87 ^a	1.44	6.532E-2	8.20
351.89 ± 0.01	1.48	2.953E0	0.20
371.80 ± 0.31	1.44	1.567E-2	16.50
386.83 ± 0.05	1.49	1.765E-2	2.10
388.92 ± 0.04	1.49	2.375E-2	1.60
401.84 ± 0.04	1.49	2.088E-2	2.75

Table 4.1 (cont'd)

Energy ± Error (keV)	FWHM (keV)	Count Rate (cps)	Error (%)
404.89 ± 0.24	1.49	1.333E-2	11.05
405.74 ± 0.32	1.49	6.658E-3	20.45
426.83 ± 0.32	2.24	8.352E-3	23.00
444.92 ± 0.26	1.53	3.961E-3	9.75
454.75 ± 0.05	1.46	1.412E-2	2.40
461.80 ± 0.15	1.94	1.119E-2	3.95
469.68 ± 0.09	1.63	5.506E-3	3.35
474.60 ± 0.12	1.63	4.379E-3	3.25
477.12 ± 0.00	1.63	3.245E-3	61.55
480.55 ± 0.05	1.63	1.908E-2	1.40
487.16 ± 0.04	1.63	2.200E-2	2.00
509.96 ± 0.22	2.36	2.762E-2	5.40
511.89 ± 0.36	2.36	2.762E-2	6.90
533.78 ± 0.09 ^a	1.43	1.071E-2	4.70
543.56 ± 0.20 ^a	1.81	4.279E-3	9.90
547.21 ± 0.40 ^a	1.81	1.130E-2	18.40
572.70 ± 0.37	1.84	2.676E-3	16.05
580.32 ± 0.04	1.60	1.421E-2	2.50
595.85 ± 24	1.51	6.539E-3	9.35
609.27 ± 0.01 ^a	1.66	1.789E00	0.30
615.98 ± 0.18 ^a	1.66	1.255E-2	29.05
633.26 ± 0.27	1.99	1.855E-2	18.50
639.57 ± 0.39	1.99	1.167E-2	19.35
649.34 ± 0.20	1.41	1.239E-2	12.60
665.42 ± 0.02	1.67	4.716E-2	0.80
683.13 ± 0.29	1.41	1.388E-3	18.35
688.54 ± 0.53	1.81	1.868E-2	21.80
698.23 ± 0.54 ^a	1.84	1.200E-2	21.25
703.22 ± 0.07	1.57	1.498E-2	4.80
710.84 ± 0.60	1.66	2.270E-3	31.30
719.83 ± 0.05	1.68	1.175E-2	2.95
733.99 ± 0.31	1.73	1.260E-2	15.70

Table 4.1 (cont'd)

Energy ± Error (keV)	FWHM (keV)	Count Rate (cps)	Error (%)
742.54 ± 0.06	1.97	1.504E-2	2.65
752.78 ± 0.14	1.69	3.518E-3	5.65
766.28 ± 0.07	1.77	1.449E-2	1.90
768.37 ± 0.01	1.77	1.476E-1	0.95
785.97 ± 0.03	1.86	3.798E-2	0.95
799.48 ± 0.34	1.79	9.068E-3	15.40
806.28 ± 0.02	1.79	3.475E-2	1.15
815.05 ± 0.43	1.86	9.349E-3	14.45
821.28 ± 0.11	1.86	4.470E-3	3.40
826.13 ± 0.13	1.86	4.003E-3	4.85
832.06 ± 0.10	1.86	6.085E-3	3.70
839.10 ± 0.03	1.86	2.037E-2	2.10
846.80 ± 0.30	1.43	1.648E-2	20.40
904.27 ± 0.20	1.50	1.170E-2	11.35
934.09 ± 0.02	1.86	7.638E-2	0.55
945.99 ± 0.27	0.90	4.388E-3	19.25
964.10 ± 0.07	1.90	9.339E-3	3.00
1001.04 ± 0.03	1.91	2.356E-2	1.30
1032.24 ± 0.30	2.42	1.528E-2	11.00
1048.42 ± 0.07 ^a	1.19	8.252E-3	13.35
1051.92 ± 0.09 ^a	1.19	6.903E-3	5.35
1069.95 ± 0.10	1.80	6.103E-3	4.40
1103.92 ± 0.17	2.47	3.124E-3	7.80
1120.21 ± 0.01 ^a	1.98	3.220E-1	0.25
1133.76 ± 0.15	2.00	4.588E-3	4.70
1155.12 ± 0.02	2.01	3.682E-2	0.80
1173.08 ± 0.32	2.21	1.721E-3	11.90
1182.01 ± 0.07	2.11	5.782E-2	3.35
1207.62 ± 0.09	2.05	6.660E-2	2.80
1217.36 ± 0.38	1.25	4.684E-3	22.90
1218.89 ± 0.33	1.25	6.578E-3	20.30
1238.07 ± 0.01	2.06	8.4812E-1	0.40

Table 4.1 (cont'd)

Energy \pm Error (keV)	FWHM (keV)	Count Rate (cps)	Error (%)
1253.39 \pm 0.16	2.95	5.620E-2	2.10
1274.62 \pm 0.29	2.09	1.1068E-2	10.75
1280.95 \pm 0.03	2.09	2.0468E-1	1.35
1303.77 \pm 0.23	1.95	1.3014E-2	8.60
1317.18 \pm 0.25	1.97	1.0301E-2	11.20
1377.82 \pm 0.01	2.14	6.1852E-1	0.55
1385.49 \pm 0.04	2.14	1.0601E-1	1.10

^aA satisfactory χ^2 could not be obtained, even though the peaks were allowed to vary individually. Moreover, a search for hidden peaks among the residuals revealed no additional peaks.

^bA less than optimum peak width was used when a large number of neighboring and overlapping peaks were present. All other values represent a good fit.

Table 4.2. Detected Peaks in a Sample of Ore Containing Uranium, Actinium, and Thorium Series in Secular Radioactive Equilibrium

Energy ± Error (keV)	FWHM (keV)	Count Rate (cps)	Error (%)
37.85 ± 0.17 ^{a,b}	1.15	3.6963E-01	10.35
39.90 ± 0.13 ^{a,b}	1.15	4.2541E-01	7.50
42.69 ± 0.60 ^{a,b}	1.15	6.9917E-02	34.75
46.50 ± 0.30 ^b	1.06	1.0051E-01	33.20
57.62 ± 0.08	1.04	1.2120E-01	6.05
63.34 ± 0.13	1.19	1.9834E-01	7.05
74.95 ± 0.03 ^{a,b}	1.15	5.8817E 00	1.75
77.28 ± 0.02 ^{a,b}	1.15	9.7086E 00	1.20
81.40 ± 0.50 ^{a,b}	1.29	1.2496E-01	24.75
84.76 ± 0.05 ^{a,b}	1.29	1.2028E 00	4.40
87.71 ± 0.02 ^{a,b}	1.29	4.0596E 00	3.20
90.53 ± 0.02 ^{a,b}	1.29	3.1332E 00	3.30
93.91 ± 1.50 ^{a,b}	1.17	1.1891E 00	25.75
94.17 ± 1.19 ^{a,b}	1.17	1.6449E 00	22.95
100.51 ± 0.06	1.23	6.9065E-01	2.05
106.64 ± 0.17 ^a	1.49	1.0542E 00	3.90
110.16 ± 2.53 ^a	1.49	3.3004E-01	4.35
110.26 ± 15.23 ^a	1.49	6.1544E-02	98.50
116.90 ± 0.05	1.16	3.5168E-01	4.00
129.07 ± 0.02	1.16	1.3546E 00	0.95
131.51 ± 0.15	1.16	1.0935E-01	5.65
140.86 ± 0.40	1.06	2.4933E-02	26.65
145.85 ± 0.16	1.13	7.4840E-02	8.50
153.99 ± 0.04	1.16	4.2521E-01	2.00
166.34 ± 0.16	0.95	5.1180E-02	10.00
176.49 ± 0.19	0.51	1.4198E-02	16.60
186.04 ± 0.06	1.29	2.8243E-01	2.75
191.29 ± 0.13	1.11	5.1167E-02	13.90
199.41 ± 0.08	1.19	1.1774E-01	3.95
204.11 ± 0.28	1.19	4.6231E-02	6.65

Table 4.2 (cont'd)

Energy ± Error (keV)	FWHM (keV)	Count Rate (cps)	Error (%)
209.24 ± 0.01	1.19	1.7416E 00	0.65
215.94 ± 0.10	1.16	1.2103E-01	5.30
233.29 ± 0.32	1.07	2.5145E-02	21.20
238.62 ± 0 ^a	1.22	1.9397E 01	0.20
240.93 ± 0.04 ^a	1.22	1.8534E 00	1.15
241.92 ± 0.21 ^a	1.22	2.6430E-01	10.05
252.66 ± 0.12	1.16	7.6698E-02	5.05
270.22 ± 0.01	1.25	1.1696E 00	0.65
277.33 ± 0.02	1.23	6.9092E-01	1.35
278.84 ± 0.22	1.23	5.4962E-02	4.50
288.10 ± 0.05	1.24	1.2300E-01	2.50
295.16 ± 0.03	1.23	3.7842E-01	1.70
300.03 ± 0.45	1.23	7.1159E-01	102.35
300.26 ± 1.09	1.23	2.6115E-01	102.35
321.62 ± 0.12	1.21	5.1021E-02	6.80
327.97 ± 0.01 ^b	1.28	8.5833E-01	0.75
332.37 ± 0.05 ^b	1.28	1.0386E-01	2.00
338.29 ± 0.01 ^b	1.29	3.3260E 00	0.35
340.86 ± 0.06 ^b	1.29	1.0516E-01	2.45
351.89 ± 0.02	1.30	6.2441E-01	0.75
377.37 ± 0.48	1.01	5.5626E-02	19.60
387.04 ± 0.44	1.70	2.2001E-02	12.60
409.45 ± 0.02	1.29	4.1027E-01	1.20
415.32 ± 0.32	1.29	1.9400E-02	8.10
440.50 ± 0.17	0.93	2.0315E-02	9.10
452.86 ± 0.06	1.29	7.5583E-02	3.20
462.99 ± 0.02	1.36	8.1940E-01	0.60
473.53 ± 0.61	1.57	1.2274E-02	24.05
478.26 ± 0.26	1.57	3.1449E-02	14.15
503.86 ± 0.19	1.33	2.3646E-02	10.90
510.74 ± 0.03 ^a	1.42	1.2793E 00	1.70

Table 4.2 (cont'd)

Energy ± Error (keV)	FWHM (keV)	Count Rate (cps)	Error (%)
523.26 ± 0.61	1.41	1.0562E-02	24.70
546.40 ± 0.17	1.15	2.5278E-02	13.45
549.55 ± 1.13	1.15	1.4875E-02	78.70
550.01 ± 2.63	1.15	5.2149E-03	102.35
562.52 ± 0.05	1.39	1.5086E-01	2.15
571.42 ± 0.34	1.82	3.4806E-02	6.95
583.21 ± 0.01	1.42	4.3819E 00	0.20
609.27 ± 0.03	1.46	3.9665E-01	1.15
616.06 ± 0.50	1.02	7.2584E-03	29.45
665.90 ± 0.40	1.77	1.5339E-02	17.60
701.84 ± 0.26	1.91	2.6778E-02	8.05
707.55 ± 0.27	1.91	2.9936E-02	4.85
727.33 ± 0.02	1.54	9.3788E-01	0.55
755.37 ± 0.07	1.52	1.1173E-01	2.45
763.42 ± 0.07	1.42	6.4026E-02	3.70
768.37 ± 0.15	1.42	2.6048E-02	4.95
772.15 ± 0.53	1.42	8.8136E-02	53.65
772.65 ± 0.61	1.42	6.8816E-02	67.80
782.20 ± 0.08	1.45	5.4418E-02	4.75
785.48 ± 0.99	1.45	7.4389E-02	98.65
785.83 ± 1.24	1.45	5.0995E-02	102.35
795.02 ± 0.02	1.55	4.5364E-01	0.80
830.60 ± 0.09	1.58	5.3171E-02	3.55
835.80 ± 0.04	1.58	1.7216E-01	1.70
840.41 ± 0.06	1.58	9.3670E-02	2.20
847.05 ± 0.29	1.58	1.6905E-02	8.45
860.65 ± 0.02	1.56	4.8955E-01	0.75
893.48 ± 0.13	1.52	3.3213E-02	5.30
904.32 ± 0.10	1.54	6.0191E-02	3.50
911.30 ± 0.01	1.60	2.7159E 00	0.55
934.09 ± 0.28	1.72	1.6932E-02	9.65
944.03 ± 0.34 ^b	1.71	1.0695E-02	12.15

Table 4.2 (Cont'd)

Energy \pm Error (keV)	FWHM (keV)	Count Rate (cps)	Error (%)
947.92 \pm 0.29 ^b	1.71	1.2247E-02	11.30
952.29 \pm 0.18 ^b	1.71	1.5313E-02	13.15
958.70 \pm 0.16 ^b	1.62	2.5464E-02	6.75
964.87 \pm 0.03 ^b	1.62	4.5824E-01	1.10
969.08 \pm 0.01 ^b	1.62	1.5496E 00	0.75
976.17 \pm 0.64	1.92	3.8083E-03	25.00
982.40 \pm 0.38	1.92	8.8773E-03	11.95
988.27 \pm 0.21	1.92	1.6042E-02	10.25
1001.04 \pm 0.27	1.69	1.6600E-02	13.85
1003.72 \pm 6.18	1.69	2.1894E-03	102.35
1004.59 \pm 0.99	1.69	1.5260E-02	54.35
1016.47 \pm 0.45	1.05	4.5116E-03	42.65
1017.73 \pm 1.61	1.05	1.2340E-03	44.90
1033.39 \pm 0.20	1.81	1.7980E-02	9.50
1040.08 \pm 0.51	1.81	8.7579E-03	12.60
1065.17 \pm 0.14	1.51	3.2338E-02	5.50
1078.78 \pm 0.10	1.74	4.5209E-02	3.40
1094.10 \pm 0.14 ^a	2.10	5.8744E-02	3.90
1110.60 \pm 0.10	1.68	3.9278E-02	3.55
1120.39 \pm 0.08	1.61	7.1589E-02	2.80
1122.94 \pm 0.22	1.61	1.8484E-02	4.55
1153.88 \pm 0.32	2.17	1.6865E-02	7.00
1164.77 \pm 0.44	1.29	4.1003E-03	26.05
1168.72 \pm 0.49	1.29	4.2064E-03	25.60
1177.54 \pm 0	1.06	9.6006E 00	0.25
1178.67 \pm 0.02	1.06	1.3705E 00	0.70

^aA satisfactory χ^2 could not be obtained, even though the peaks were allowed to vary individually. Moreover, a search for hidden peaks among the residuals revealed no additional peaks.

^bA less than optimum peak width was used when a large number of neighboring and overlapping peaks were present. All other values represent a good fit.

Table 4.3. Energy and Quantum Yield of Selected Nuclides in the Uranium Series

Energy (keV)	Quantum Yield	Energy (keV)	Quantum Yield
Th-234		Bi-214	
63.34	4.05 E-2	303.06	8.00 E-4
		333.97	6.00 E-4
Pa-234		338.29	4.00 E-4
131.49	3.98 E-5	386.83	5.17 E-3
733.99	1.04 E-4	388.92	4.49 E-3
945.99	4.14 E-4	405.74	1.56 E-3
		454.75	2.89 E-3
Pa-234m		462.24	2.25 E-3
258.44	3.31 E-4	469.86	1.18 E-3
742.54	5.00 E-4	474.60	1.06 E-3
766.28	3.68 E-3	543.56	7.67 E-4
786.27	6.60 E-4	572.70	1.00 E-3
1001.04	9.20 E-3	609.27	4.33 E-1
		615.98	9.33 E-4
U-234		633.26	6.10 E-4
53.18	1.18 E-3	639.57	2.96 E-4
		649.34	5.90 E-4
Th-230		665.42	1.25 E-2
67.67	3.63 E-3	683.13	6.74 E-4
144.24	2.76 E-4	698.23	3.34 E-4
		703.22	3.93 E-3
Ra-226		710.84	7.11 E-4
186.04	5.05 E-2	719.83	3.64 E-3
		734.30	4.99 E-4
Pb-214		752.97	1.25 E-3
52.14	1.06 E-2	768.37	4.97 E-2
241.92	8.39 E-2	785.97	8.60 E-3
259.09	5.48 E-3	806.28	1.04 E-2
274.75	3.87 E-3	815.05	4.34 E-4
295.16	1.15 E-3	821.28	1.30 E-3
314.34	8.53 E-4	826.13	4.59 E-4
351.89	3.89 E-1	832.06	1.85 E-4
461.92	2.25 E-3	839.10	7.96 E-3
480.55	3.82 E-3	934.09	2.95 E-2
487.16	3.62 E-3	964.10	3.23 E-3
533.78	2.53 E-3	1032.24	1.18 E-3
543.56	1.17 E-3	1051.92	2.82 E-3
580.32	3.32 E-3	1069.95	1.98 E-3
785.97	8.60 E-3	1103.92	1.39 E-3
904.27	1.14 E-3	1120.21	1.46 E-1
		1133.76	2.46 E-3
Bi-214		1155.12	1.60 E-2
273.53	3.87 E-3	1173.08	7.21 E-4
281.09	9.14 E-4	1207.62	4.30 E-3
286.12	3.00 E-4	1238.07	5.98 E-2

Table 4.3 (cont'd)

Energy (keV)	Quantum Yield		Energy (keV)	Quantum Yield
Bi-214		Po-214		
1280.95	1.33 E-2		799.48	4.00 E-4
1303.77	1.04 E-3			
1377.82	4.91 E-2	Pb-210		
1385.49	7.76 E-3		46.50	4.1 E-2

Table 4.4. Energy and Quantum Yield of Selected Nuclides in the Actinium Series

Energy (keV)	Quantum Yield		Energy (keV)	Quantum Yield
U-235		Fr-223		
109.15	1.55 E-2		49.8	4.63 E-2
115.20	1.18 E-3			
140.76	1.74 E-3	Ra-223		
143.82	1.05 E-1		123.75	1.00 E-2
163.35	4.77 E-2		144.24	5.86 E-2
185.72	5.61 E-1		154.25	7.22 E-2
195.85	6.73 E-3		158.39	6.05 E-3
202.04	8.64 E-3		269.41	1.50 E-1
205.27	4.87 E-2		323.84	3.69 E-2
221.38	1.23 E-3		333.84	4.90 E-3
240.93	7.85 E-4		338.29	1.29 E-2
246.83	6.17 E-4		371.80	4.40 E-3
			444.92	9.9 E-2
Th-231		Rn-219		
163.16	1.09 E-2		130.75	9.66 E-3
Pa-231			271.20	1.20 E-1
302.64	3.62 E-2		401.84	7.98 E-2
Th-227		Pb-211		
49.95	7.67 E-2		404.89	7.72 E-2
113.08	6.60 E-3		426.90	1.74 E-2
206.10	3.59 E-3		832.06	3.27 E-2
210.72	1.10 E-2			
235.90	1.10 E-1	Bi-211		
250.07	3.30 E-3		351.89	1.33 E-1
256.18	7.75 E-2			
281.09	1.32 E-3			
286.12	6.90 E-3			
299.93	3.89 E-2			
304.55	9.35 E-3			
314.34	4.40 E-3			
329.80	3.45 E-2			
333.97	5.11 E-4			

Table 4.5. Energy and Quantum Yield of Selected Nuclides
in the Thorium-232 Series

Energy (keV)	Quantum Yield	Energy (keV)	Quantum Yield
Ac-228		Ac-228	
129.07	1.827 E-2	969.08	1.648 E-1
140.86	3.798 E-4	976.17	4.197 E-4
145.85	1.120 E-3	988.27	1.580 E-3
184.60	1.092 E-3	1016.47	6.161 E-4
191.29	9.659 E-4	1033.39	2.046 E-3
199.41	2.465 E-3	1065.17	3.830 E-3
204.11	9.080 E-4	1153.88	2.644 E-3
209.24	3.733 E-2	1164.77	5.523 E-4
270.22	3.300 E-2		
278.84	1.458 E-3	Th-228	
321.62	1.777 E-3	131.51	1.465 E-3
327.97	2.888 E-2	215.94	2.712 E-3
332.37	3.391 E-3		
338.29	1.220 E-1	Pb-212	
340.86	3.761 E-3	176.49	2.754 E-4
377.37	1.830 E-3	238.62	4.694 E-1
409.45	1.802 E-2	300.03	2.871 E-2
416.10	4.469 E-4	415.32	4.469 E-4
440.50	9.880 E-4		
462.99	4.213 E-2	Bi-212	
474.60	3.000 E-4	39.90	8.640 E-3
478.26	1.417 E-3	153.99	7.634 E-3
503.86	1.219 E-3	288.10	3.545 E-3
523.26	7.508 E-4	295.16	4.950 E-3
546.40	1.524 E-3	327.97	1.400 E-3
562.52	9.024 E-3	452.86	3.705 E-3
571.42	2.065 E-3	473.53	1.997 E-4
616.06	4.512 E-4	727.33	6.739 E-3
665.90	3.917 E-4	893.48	3.203 E-3
701.84	2.114 E-3	952.29	1.489 E-3
707.55	2.151 E-3	1078.78	5.332 E-3
727.00	8.250 E-3		
755.37	9.167 E-3	Tl-208	
772.15	1.297 E-2	233.29	6.180 E-4
782.20	4.600 E-3	252.66	1.963 E-3
795.02	3.838 E-2	277.33	1.944 E-2
830.60	4.808 E-3	510.74	7.018 E-2
835.80	1.538 E-2	583.21	2.773 E-1
840.41	8.835 E-3	763.42	5.338 E-3
904.32	6.159 E-3	860.65	4.528 E-2
911.30	2.652 E-1	982.40	9.239 E-4
944.03	1.134 E-3	1004.59	2.011 E-3
947.92	9.748 E-4	1094.10	7.046 E-3
958.70	2.838 E-3		
964.87	4.964 E-2	Ra-224	
		240.98	4.70 E-2

Table 4.6. Energy and Quantum Yield of Nuclides in the Uranium Series: Comparison of Values Measured in This Study with Those Previously Reported^a

Nuclide	Energy (keV)	Quantum Yield	References
²³⁴ Th	63.34	4.05 E-2	*
²³⁴ Th/ ²³⁴ Pa	63.30/63.40	5.69 E-2/6.64 E-5	27
²³⁴ Th	62.92/63.35	4.6 E-3/4.7 E-2	13
²³¹ Pa/ ²³⁴ Th	63.3	--	15
²³⁴ Pa	63.4	2.8 E-2	2
²³⁴ Th	63.1	--	5
²³⁴ Th	63.28	--	26
²³⁴ Th	92.75	1.63 E-2	*
²³⁴ Th	92.30/92.8	3.15 E-2/3.55 E-2	27
²³⁴ Th	92.4	--	5
²³⁴ Th	92.0/92.38/92.80	5 E-4/1.45 E-1/3.38 E-2	13
²³⁴ Pa	131.49	3.98 E-5	*
	131.00	--	1
	131.00	4.74 E-4	27
	132.9	7.00 E-4	13
²³⁴ Pa	733.99	1.04 E-4	*
	733.39	1.06 E-4	27
²³⁴ Pa	945.99	4.14 E-4	*
	946.30	--	2
	946.04	--	15
	946.07	3.55 E-4	27
^{234m} Pa	258.44	3.31 E-4	*
	258.23	7.30 E-4	27
	258.23	--	2
^{234m} Pa	742.54	5.00 E-4	*
	742.79	9.50 E-4	27
^{234m} Pa	766.28	3.68 E-3	*
	766.39	3.13 E-3	27
^{234m} Pa	786.27	6.60 E-4	*
	786.30	5.50 E-4	27
^{234m} Pa	1001.04	9.20 E-3	*
	1001.10	8.28 E-3	27
²³⁴ U	53.18	1.18 E-3	*
	53.30	1.18 E-3	27

^aThe values measured in this investigation are followed by an asterisk in the reference column.

Table 4.6 (Continued)

Nuclide	Energy (keV)	Quantum Yield	References
^{230}Th	67.67	3.63 E-3	*
	67.8	3.81 E-3	27
	67.7	3.73 E-3	19
^{230}Th	144.24	2.76 E-4	*
	142.00	4.51 E-4	27
	143.87	4.83 E-4	19
^{226}Ra	186.04	5.05 E-2	*
	186.00	3.90 E-2	21, 27
	186.14	4.00 E-2	1, 14
^{214}Pb	52.14	1.06 E-2	*
	53.23	2.2 E-2	21
	53.0	~1. E-2	1
^{214}Pb	241.92	8.39 E-2	*
	241.92	7.60 E-2	21
	241.97	--	30
	242.0	4.0 E-2	1
^{214}Pb	259.09	5.48 E-3	*
	258.82	8.0 E-3	21
^{214}Pb	274.75	3.87 E-3	*
	274.80	7.0 E-3	21
^{214}Pb	295.16	1.15 E-1	*
	295.22	1.89 E-1	21
	295.00	1.90 E-1	1
^{214}Pb	314.34	8.53 E-4	*
	314.20	8.00 E-4	21
^{214}Pb	351.89	3.89 E-1	*
	351.99	3.63 E-1	21
	352.00	3.60 E-1	1
^{214}Pb	461.92	2.25 E-3	*
	462.10	1.70 E-3	21
^{214}Pb	480.55	3.82 E-3	*
	480.50	3.40 E-3	21
^{214}Pb	487.16	3.62 E-3	*
	487.25	3.30 E-3	21
^{214}Pb	533.78	2.53 E-3	*
	533.80	1.7 E-3	21
^{214}Pb	543.56	1.17 E-3	*
	543.50	1.0 E-3	21
^{214}Pb	580.32	3.32 E-3	*
	580.30	3.60 E-3	21

Table 4.6 (Continued)

Nuclide	Energy (keV)	Quantum Yield	References
^{214}Pb	785.97	8.60 E-3	*
	785.95	8.60 E-3	21
^{214}Pb	904.27	1.14 E-3	*
$^{214}\text{Pb}/^{214}\text{Bi}$	904.10	5.9 E-3/7.0 E-4	21
^{214}Bi	273.53	3.87 E-3	*
^{214}Bi	273.50	8.00 E-4	21
^{214}Bi	281.09	9.14 E-4	*
	281.10	6.00 E-4	21
^{214}Bi	286.12	3.00 E-4	*
^{214}Bi	286.90	3.00 E-4	21
^{214}Bi	303.06	8.00 E-4	*
^{214}Bi	303.0	8.00 E-4	21
^{214}Bi	333.97	6.00 E-4	*
^{214}Bi	334.30	6.00 E-4	21
^{214}Bi	338.29	4.00 E-4	*
^{214}Bi	338.50	4.00 E-4	21
^{214}Bi	386.83	5.17 E-3	*
^{214}Bi	386.80	3.10 E-3	21
^{214}Bi	388.92	4.49 E-3	*
	388.80	3.70 E-3	21
^{214}Bi	405.74	1.56 E-3	*
^{214}Bi	405.90	1.50 E-3	21
^{214}Bi	454.75	2.89 E-3	*
^{214}Bi	455.00	2.80 E-3	21
^{214}Bi	462.24	2.25 E-3	*
^{214}Bi	462.10	2.10 E-3	21
^{214}Bi	469.86	1.18 E-3	*
^{214}Bi	470.60	1.30 E-3	21
^{214}Bi	474.60	1.06 E-3	*
^{214}Bi	474.6	7.0 E-4	21
^{214}Bi	543.56	7.67 E-4	*
^{214}Bi	543.5	1.0 E-3	21
^{214}Bi	572.70	1.0 E-3	*
^{214}Bi	572.60	6.0 E-4	21
^{214}Bi	609.27	4.33 E-1	*
^{214}Bi	609.37	4.28 E-1	21
	609.0	4.7 E-1	1
^{214}Bi	615.98	9.33 E-4	*
	615.80	9.00 E-4	21

Table 4.6 (Continued)

Nuclide	Energy (keV)	Quantum Yield	References
^{214}Bi	633.26	6.10 E-4	*
^{214}Bi	633.60	5.0 E-4	21
^{214}Bi	639.57	2.96 E-4	*
^{214}Bi	639.0	3.0 E-4	21
^{214}Bi	649.34	5.90 E-4	*
^{214}Bi	649.40	5.0 E-4	21
^{214}Bi	665.42	1.25 E-2	*
^{214}Bi	665.60	1.40 E-2	21
	665.0	2.3 E-2	1
^{214}Bi	683.13	6.74 E-4	*
^{214}Bi	683.30	8.0 E-4	21
^{214}Bi	698.23	3.34 E-4	*
^{214}Bi	698.40	7.0 E-4	21
^{214}Bi	703.22	3.93 E-3	*
^{214}Bi	703.10	4.70 E-3	21
^{214}Bi	710.84	7.11 E-4	*
^{214}Bi	710.8	6.0 E-4	21
^{214}Bi	719.83	3.64 E-3	*
^{214}Bi	719.90	3.80 E-3	21
^{214}Bi	734.30	4.99 E-4	*
	734.30	3.0 E-4	21
^{214}Bi	752.97	1.25 E-3	*
	753.0	1.1 E-3	21
^{214}Bi	768.37	4.97 E-2	*
^{214}Bi	768.40	8.0 E-4	21
$^{214}\text{Bi}/^{214}\text{Pb}$	768.40	4.8 E-2/8.0 E-4	27
	769.0	5.3 E-2	1
^{214}Bi	785.97	8.60 E-3	*
^{214}Bi	785.95	1.05 E-2	21
^{214}Bi	786.10	2.90 E-3	27
	787.0	1.2 E-2	1
^{214}Bi	806.28	1.04 E-2	*
^{214}Bi	806.20	1.10 E-2	21
	805.0	1.5 E-2	1
^{214}Bi	815.05	4.34 E-4	*
	815.0	4.0 E-4	21
^{214}Bi	821.28	1.30 E-3	*
	821.20	1.6 E-3	21
^{214}Bi	826.13	4.59 E-4	*
	826.0	1.3 E-3	21

Table 4.6 (Continued)

Nuclide	Energy (keV)	Quantum Yield	References
^{214}Bi	832.06	1.85 E-4	*
	832.0	3.0 E-4	21
^{214}Bi	839.10	7.96 E-3	*
	839.20	5.9 E-3	21
^{214}Bi	934.09	2.95 E-2	*
	934.0	3.1 E-2	21
	935.0	3.3 E-2	1
^{214}Bi	964.10	3.23 E-3	*
	964.10	3.7 E-3	21
^{214}Bi	1032.24	1.18 E-3	*
	1032.5	7.0 E-4	21
^{214}Bi	1051.92	2.82 E-3	*
	1052.00	3.3 E-3	21
^{214}Bi	1069.95	1.98 E-3	*
	1070.00	2.60 E-3	21
^{214}Bi	1103.92	1.39 E-3	*
	1104.0	1.6 E-3	21
^{214}Bi	1120.21	1.46 E-1	*
	1120.40	1.50 E-1	21
	1120.0	1.6 E-1	1
^{214}Bi	1133.76	2.46 E-3	*
	1133.80	2.50 E-3	21
^{214}Bi	1155.12	1.60 E-2	*
	1155.30	1.70 E-2	21
	1155.0	1.80 E-2	1
^{214}Bi	1173.08	7.21 E-4	*
	1172.90	3.0 E-4	21
^{214}Bi	1207.62	4.30 E-3	*
	1207.80	4.70 E-3	21
^{214}Bi	1238.07	5.98 E-2	*
	1238.2	6.1 E-2	21
^{214}Bi	1280.95	1.33 E-2	*
	1281.10	1.50 E-2	21
^{214}Bi	1303.77	1.04 E-3	*
	1303.80	1.10 E-3	21
^{214}Bi	1377.82	4.91 E-2	*
	1377.70	4.30 E-2	21
^{214}Bi	1385.49	7.76 E-3	*
	1385.40	8.0 E-3	21
^{214}Po	799.48	4.0 E-4	*
^{214}Po	799.00	1.4 E-4	27

Table 4.6 (Continued)

Nuclide	Energy (keV)	Quantum Yield	References
^{210}Pb	46.50	4.10 E-2	*
	46.52	7.30 E-2	21
	46.52	4.10 E-2	27
	47.0	4.10 E-2	1

Table 4.7. Energy and Quantum Yield of Nuclides in the Actinium Series:
Comparison of Values Measured in This Study with
Those Previously Reported^a

Nuclide	Energy (keV)	Quantum Yield	References
²³⁵ U	109.15	1.55 E-2	*
	110.0		20
	109.145		29
	109.12		15
²³⁵ U	115.20	1.18 E-3	*
	115.20		15
²³⁵ U	140.76	1.74 E-3	*
	140.75	2.08 E-3	27
	140.758		29
	140.75		15
²³⁵ U	143.82	1.05 E-1	*
	143.78		15
	143.753		29
	143.0	1.1 E-1	1
	143.77	1.07 E-1	27
²³⁵ U	163.35	4.77 E-2	*
	163.37	4.85 E-2	27
	163.349		29
	163.363		15
²³⁵ U	185.72	5.61 E-1	*
	185.712		29
	185.72	5.61 E-1	27
	185.718		15
	185.0	5.4 E-1	1
²³⁵ U	195.85	6.73 E-3	*
	194.938		29
	194.94	6.15 E-3	27
	194.94		15
²³⁵ U	202.04	8.64 E-3	*
	202.105		29
	202.10	1.07 E-2	27
	202.13		15
²³⁵ U	205.27	4.87 E-2	*
	205.312		29
	205.33	4.87 E-2	27
	205.311		15

^aThe values measured in this investigation are followed by an asterisk in the reference column.

Table 4.7 (Continued)

Nuclide	Energy (keV)	Quantum Yield	References
^{235}U	221.38	1.23 E-3	*
	221.397		29
	221.375		27
^{235}U	240.93	7.85 E-4	*
	240.93	6.40 E-4	27
	240.95		29
	240.93		15
^{235}U	246.83	6.17 E-4	*
	246.88	5.20 E-4	27
	246.59		29
	246.83		15
^{231}Th	163.64	1.09 E-2	*
	163.16	1.39 E-3	27
	163.33		20
^{231}Pa	302.50	3.62 E-2	*
	302.52	7.02 E-4	27
	302.0		20
^{227}Th	49.95	7.67 E-2	*
	50.20	8.59 E-2	27
	50.0		20
	49.9/50.1	4.4 E-2	7
^{227}Th	113.08	6.60 E-3	*
	113.1	7.7 E-3	7
	113.1	5.33 E-3	27
^{227}Th	206.10	3.59 E-3	*
	206.0	2.20 E-3	7
	206.1/206.4	2.57 E-3/3.93 E-5	27
^{227}Th	210.72	1.10 E-2	*
	210.60	9.90 E-3	7
	210.60	1.24 E-2	27
^{227}Th	235.90	1.10 E-1	*
	236.0	1.035 E-1	7
	236.00	1.14 E-1	27
^{227}Th	250.07	3.30 E-3	*
	250.1	4.90 E-3	7
	249.6/250.2/250.4	6.91 E-5/2.76 E-3/6.91 E-4	27
	250.0		15
^{227}Th	256.18	7.75 E-2	*
	256.20	6.03 E-2	7
	256.20	6.22 E-2	27

Table 4.7 (Continued)

Nuclide	Energy (keV)	Quantum Yield	References
^{227}Th	281.09	1.32 E-3	*
	281.3	1.70 E-3	7
	281.4	1.48 E-3	27
	281.0		20
	286.12	6.90 E-3	*
	286.10	1.50 E-2	7
	286.20	1.63 E-2	27
^{227}Th	299.93	3.89 E-3	*
	299.8	1.86 E-2	7
^{227}Th	304.55	9.35 E-3	*
	304.40	1.33 E-2	27
	304.40	8.90 E-3	7
^{227}Th	314.34	4.40 E-3	*
	314.8	3.90 E-3	7
	314.8	5.33 E-3	27
^{227}Th	329.80	3.45 E-2	*
	329.70	2.37 E-2	7
	329.70	2.86 E-2	27
^{227}Th	333.97	5.11 E-4	*
	334.20	8.65 E-3	7
	334.40	1.14 E-2	27
	334.02		15
^{223}Fr	49.8	4.63 E-2	*
	49.8	5.20 E-3	27
^{223}Ra	122.75	1.00 E-2	*
	122.30	1.33 E-2	8
^{223}Ra	144.24	5.86 E-2	*
	144.19	3.13 E-2	8
^{223}Ra	154.25	7.22 E-2	*
	154.18	5.23 E-2	8
^{223}Ra	158.39	6.05 E-3	*
	158.62	7.60 E-3	8
^{223}Ra	269.41	1.50 E-1	*
	269.41	1.36 E-1	8
^{223}Ra	323.84	3.69 E-2	*
	323.88	3.60 E-2	8
^{223}Ra	333.84	4.90 E-3	*
	333.80	1.24 E-3	8
^{223}Ra	338.29	1.29 E-2	*
	338.30	2.59 E-2	8

Table 4.7 (Continued)

Nuclide	Energy (keV)	Quantum Yield	References
^{223}Ra	371.80	4.40 E-3	*
	371.50	5.40 E-3	8
^{223}Ra	444.92	9.90 E-2	*
	444.92	1.27 E-2	8
^{219}Rn	130.75	9.66 E-3	*
	130.70	1.04 E-3	9
^{219}Rn	271.20	1.20 E-1	*
	271.20	9.93 E-2	9
^{219}Rn	401.84	7.98 E-2	*
	401.80	6.48 E-2	9
^{211}Pb	404.89	7.72 E-2	*
	404.80	3.94 E-2	27
^{211}Pb	426.90	1.74 E-2	*
	426.90	1.82 E-2	27
	832.06	3.27 E-2	*
	831.80	3.21 E-2	27
^{211}Bi	351.89	1.33 E-1	*
	351.10	1.33 E-1	27

Table 4.8. Energy and Quantum Yield of Nuclides in the Thorium Series:
Comparison of Values Measured in this Study with
Those Previously Reported^a

Nuclide	Energy (keV)	Quantum Yield	References
²²⁸ Th	131.51	1.475 E-3	*
	132.0		20
	131.62		15
	132.0	2.60 E-3	27
²²⁸ Th	215.94	2.71 E-3	*
	214.0		20
	215.94		15
	217.0	2.70 E-3	27
²¹² Pb	176.49	2.75 E-4	*
	176.63	5.22 E-4	27
	176.84		15
²¹² Pb	238.62	4.69 E-1	*
	238.62		15/20
	238.63	4.46 E-1	27
²¹² Pb	300.03	2.87 E-2	*
	300.1		20
	300.08		15
	300.11	3.42 E-2	27
²¹² Pb	415.32	4.47 E-4	*
	415.2		20
	415.2	1.80 E-4	27
²¹² Bi	39.90	8.64 E-3	*
	39.85		20
	39.87	1.10 E-2	27
²¹² Bi	153.99	7.63 E-3	*
	154.0	1.01 E-4	27
²¹² Bi	288.10	3.55 E-3	*
	288.07	3.42 E-3	27
²¹² Bi	295.10	4.95 E-3	*
	294.0		20
	295.19		15
	295.10	2.41 E-4	27
²¹² Bi	327.97	1.40 E-3	*
	328.0		20
²¹² Bi	327.98		15
	327.96	1.40 E-3	27

^aThe values measured in this investigation are followed by an asterisk in the reference column.

Table 4.8 (Continued)

Nuclide	Energy (keV)	Quantum Yield	References
^{212}Bi	452.86	3.71 E-3	*
	452.91		15
	452.0		20
	452.83	3.74 E-3	27
^{212}Bi	473.53	2.00 E-4	*
	472.0		20
	473.50	4.68 E-4	27
^{212}Bi	727.33	6.74 E-2	*
	727.0	7.1 E-2	1
	727.27	6.66 E-2	27
^{212}Bi	893.48	3.20 E-3	*
	893.30		15
	893.35	3.67 E-3	27
^{212}Bi	952.29	1.49 E-3	*
	952.10	1.76 E-3	27
^{212}Bi	1078.78	5.33 E-3	*
	1078.73		15
	1078.80	5.36 E-3	27
^{208}Tl	233.29	6.18 E-4	*
	233.50	1.19 E-3	27
	233.0		20
^{208}Tl	252.66	1.96 E-3	*
	252.0		20
	252.60	2.52 E-3	27
^{208}Tl	277.33	1.94 E-2	*
	277.33		20
	277.36		15
	277.36	2.34 E-2	27
^{208}Tl	510.74	7.02 E-2	*
	510.72		20
	510.70		15
	510.72	8.10 E-2	27
^{208}Tl	583.21	2.77 E-1	*
	583.14	3.10 E-1	27
^{208}Tl	763.42	5.34 E-3	*
	763.32		15
	763.2		20
	763.30	6.05 E-3	27
^{208}Tl	860.65	4.528 E-2	*
	860.53		15
	860.0		20
	860.47	4.32 E-2	27

Table 4.8 (Continued)

Nuclide	Energy (keV)	Quantum Yield	References
²⁰⁸ Tl	982.40	9.24 E-4	*
	982.80	7.20 E-4	27
²⁰⁸ Tl	1004.59	2.01 E-3	*
	1004.00	3.60 E-3	27
²²⁴ Ra	240.98	4.70 E-2	*
	240.98		20
	240.98	3.70 E-2	27
²²⁸ Ac	129.07	1.83 E-2	*
	128.90		15
	129.0		20
	129.10	3.03 E-2	27
²²⁸ Ac	140.86	3.80 E-4	*
	141.00	5.10 E-4	27
²²⁸ Ac	145.85	1.12 E-3	*
	145.90	2.28 E-3	27
²²⁸ Ac	184.60	1.09 E-3	*
	184.0		20
	184.60	1.05 E-3	27
²²⁸ Ac	191.29	9.66 E-4	*
	191.50	1.26 E-3	27
²²⁸ Ac	199.41	2.47 E-3	*
	199.50	3.63 E-3	27
²²⁸ Ac	204.11	9.08 E-4	*
	204.10	1.77 E-3	27
²²⁸ Ac	209.24	3.73 E-2	*
	209.40	4.71 E-2	27
²²⁸ Ac	270.22	3.30 E-2	*
	270.30	3.90 E-2	27
	270.21		15
²²⁸ Ac	278.84	1.46 E-3	*
	279.00	2.40 E-3	27
²²⁸ Ac	321.62	1.78 E-3	*
	321.70	2.61 E-3	27
²²⁸ Ac	328.00	2.89 E-2	*
	328.0	3.48 E-2	27
²²⁸ Ac	332.37	3.39 E-3	*
	332.40	4.89 E-3	27
²²⁸ Ac	338.29	1.22 E-1	*
	338.296		15
	338.40	1.24 E-1	27

Table 4.8 (Continued)

Nuclide	Energy (keV)	Quantum Yield	References
^{228}Ac	340.86	3.76 E-3	*
	340.90	4.35 E-3	27
^{228}Ac	377.37	1.83 E-3	*
	377.80	3.30 E-4	27
^{228}Ac	409.45	1.80 E-2	*
	409.44		15
	409.40	2.31 E-2	27
^{228}Ac	416.10	4.47 E-4	*
	416.10	1.80 E-4	27
^{228}Ac	440.50	9.88 E-4	*
	440.30	1.50 E-3	27
^{228}Ac	462.99	4.21 E-2	*
	463.00		15
	463.00	4.80 E-2	
^{228}Ac	474.60	3.00 E-4	*
	474.60	3.00 E-4	27
^{228}Ac	478.26	1.42 E-3	*
	478.20	2.49 E-3	27
^{228}Ac	503.86	1.22 E-3	*
	503.70	2.22 E-3	27
^{228}Ac	523.26	7.51 E-4	*
	523.00	1.26 E-3	27
^{228}Ac	546.40	1.52 E-3	*
	546.30	2.28 E-3	27
^{228}Ac	562.52	9.02 E-3	*
	562.30	1.02 E-2	27
^{228}Ac	571.42	2.07 E-3	*
	570.70/572.10	1.92 E-3/1.68 E-3	27
^{228}Ac	616.06	4.51 E-4	*
	615.90	9.00 E-4	27
^{228}Ac	665.90	3.92 E-4	*
	666.30	4.80 E-4	27
^{228}Ac	701.84	2.114 E-3	*
	701.50	2.04 E-3	27
^{228}Ac	707.55	2.15 E-3	*
	707.30	1.62 E-3	27
^{228}Ac	727.08	8.29 E-3	*
	727.00	8.25 E-3	27
	755.37	9.17 E-3	*
	755.20	1.14 E-2	27
	755.29		15

Table 4.8 (Continued)

Nuclide	Energy (keV)	Quantum Yield	References
²²⁸ Ac	772.15	1.30 E-2	*
	772.10	1.68 E-2	27
²²⁸ Ac	782.20	4.60 E-3	*
	782.00	5.64 E-3	27
²²⁸ Ac	795.02	3.84 E-2	*
	794.80	5.01 E-2	27
²²⁸ Ac	830.60	4.81 E-3	*
	830.48		15
	830.40	6.39 E-3	27
²²⁸ Ac	835.80	1.54 E-2	*
	835.70		15
	835.60	1.88 E-2	27
²²⁸ Ac	840.41	8.84 E-3	*
	840.29		15
	840.20	1.02 E-2	27
²²⁸ Ac	904.32	6.16 E-3	*
	904.20	9.00 E-3	27
	904.22		15
²²⁸ Ac	911.30	2.65 E-1	*
	911.18		15
	911.10	3.00 E-1	27
²²⁸ Ac	944.03	1.13 E-3	*
	944.10	1.11 E-3	27
²²⁸ Ac	947.92	9.75 E-4	*
	948.00	1.26 E-3	27
²²⁸ Ac	958.70	2.84 E-3	*
	958.50	3.27 E-3	27
²²⁸ Ac	964.87	4.96 E-2	*
	964.80		15
	964.60	5.64 E-2	27
²²⁸ Ac	969.08	1.65 E-1	*
	968.94		15
	968.90	1.81 E-1	27
²²⁸ Ac	976.17	4.20 E-4	*
	975.90	5.40 E-4	27
²²⁸ Ac	988.27	1.58 E-3	*
	988.10	1.98 E-3	27
²²⁸ Ac	1016.47	6.16 E-4	*
	1016.70	2.55 E-4	27
²²⁸ Ac	1033.39	2.05 E-3	*
	1033.10	2.34 E-3	27

Table 4.8 (Continued)

Nuclide	Energy (keV)	Quantum Yield	References
^{228}Ac	1065.17	3.83 E-3	*
	1065.10	1.53 E-3	27
^{228}Ac	1153.88	2.64 E-3	*
	1153.60	1.65 E-3	27
^{228}Ac	1164.77	5.52 E-4	*
	1164.60	7.80 E-4	27

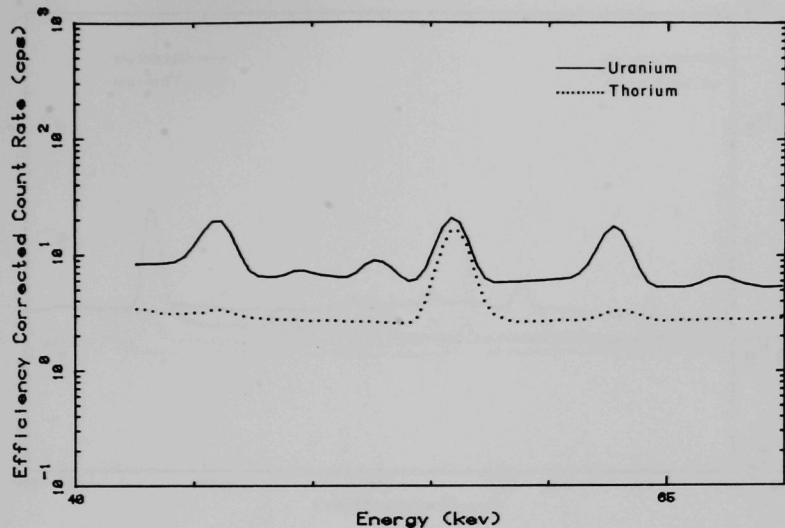


Figure 4.1. Gamma Spectra of the Uranium and Thorium Ores, 40 - 70 keV.

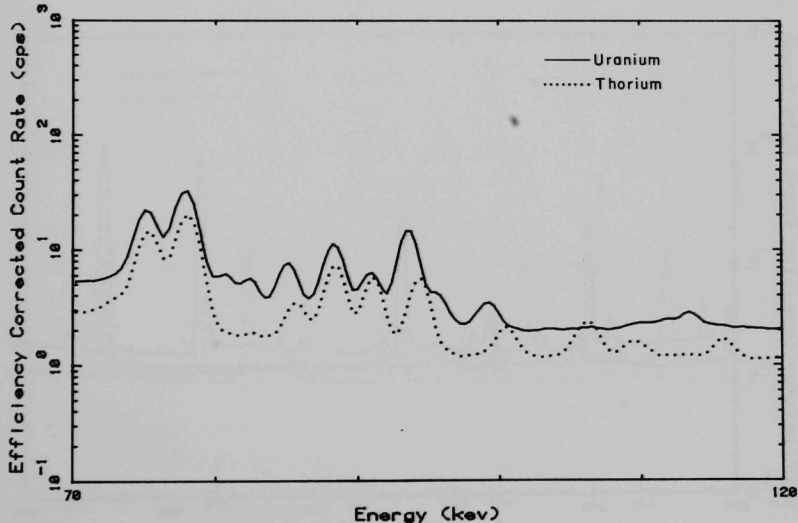


Figure 4.2. Gamma Spectra of the Uranium and Thorium Ores, 70 - 120 keV.

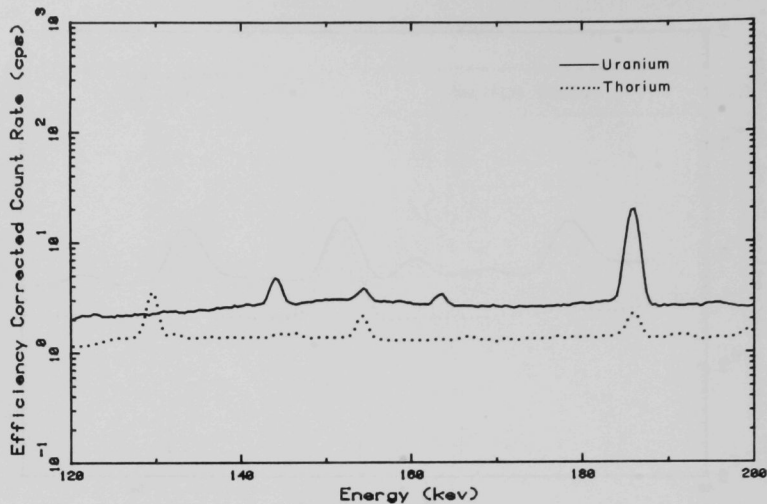


Figure 4.3. Gamma Spectra of the Uranium and Thorium Ores, 120 - 200 keV.

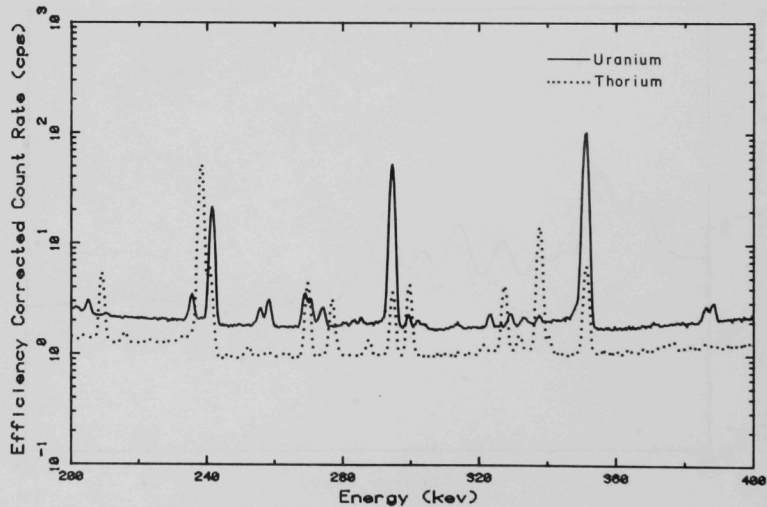


Figure 4.4. Gamma Spectra of the Uranium and Thorium Ores, 200 - 400 keV.

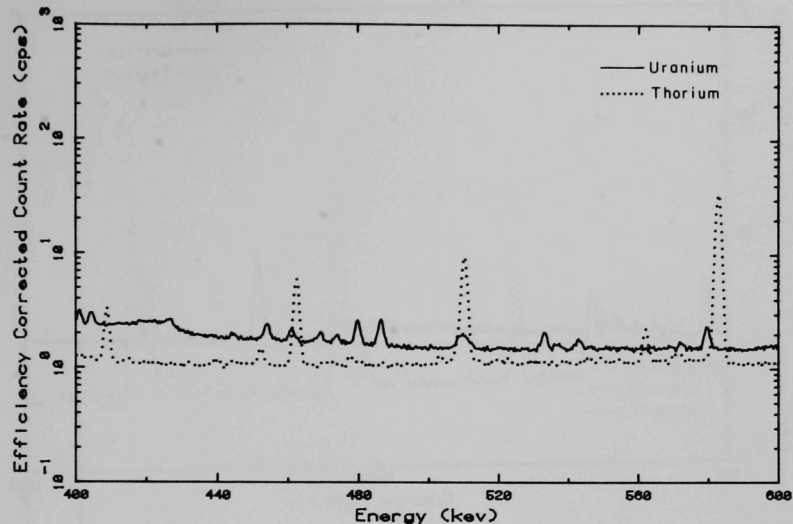


Figure 4.5. Gamma Spectra of the Uranium and Thorium Ores, 400 - 600 keV.

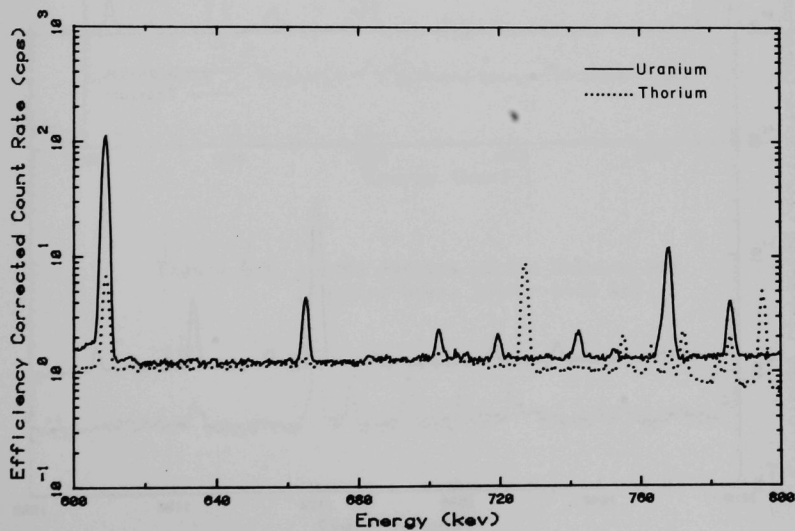


Figure 4.6. Gamma Spectra of the Uranium and Thorium Ores, 600 - 800 keV.

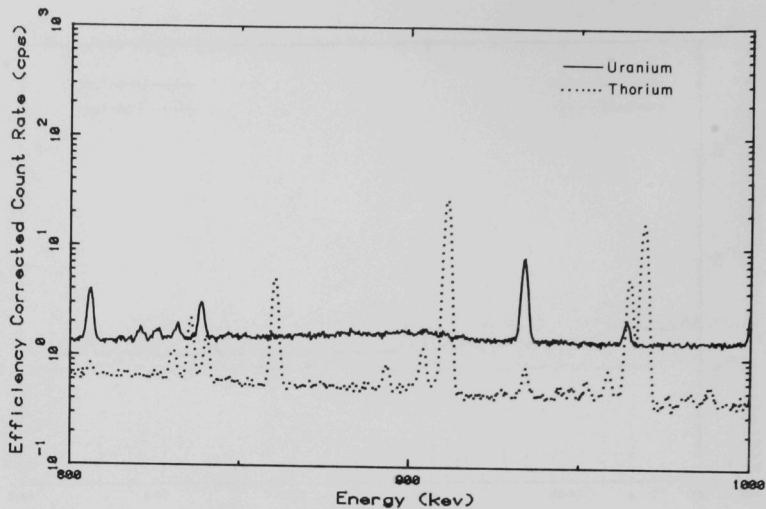


Figure 4.7. Gamma Spectra of the Uranium and Thorium Ores, 800 - 1000 keV.

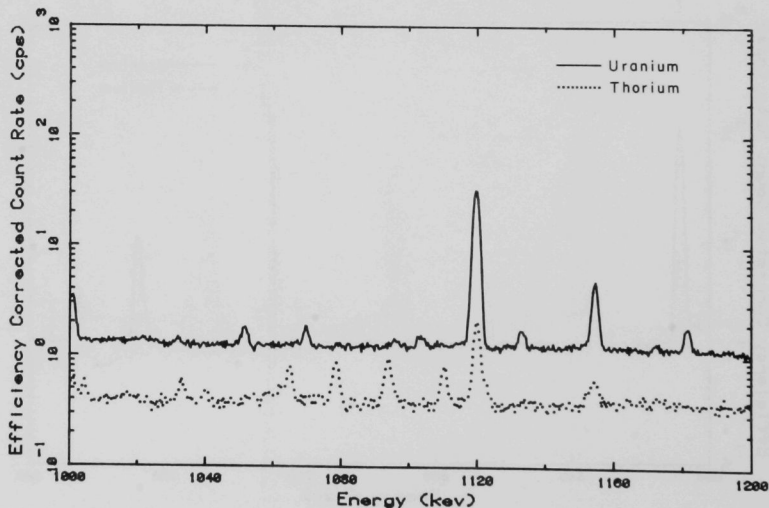


Figure 4.8. Gamma Spectra of the Uranium and Thorium Ores, 1000 - 1200 keV.

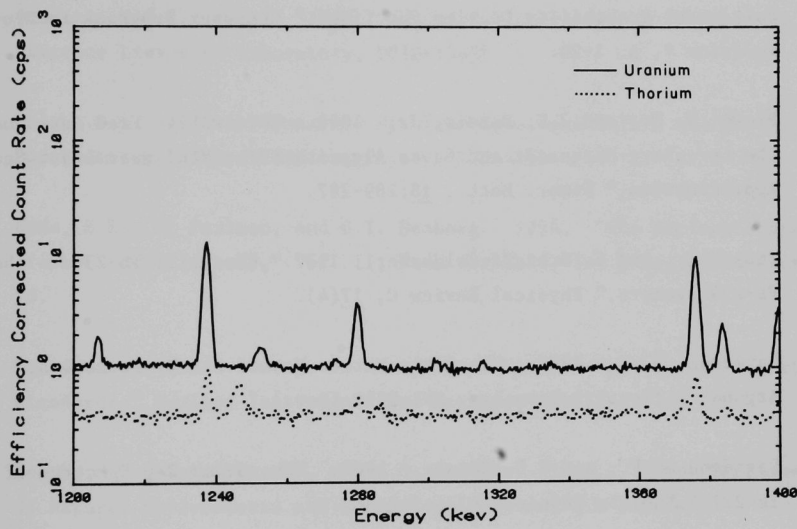


Figure 4.9. Gamma Spectra of the Uranium and Thorium Ores, 1200 - 1400 keV.

REFERENCES

1. Adams, J.A.S., and P. Gasparini. 1970. "Gamma-Ray Spectroscopy of Rocks," American Elsevier Publishing Company, Inc., New York.
2. Bjornholm, S., et al. 1968. "Energy Levels in U-234 Propagated in the β -Decay of Pa-234(UZ)," Nuclear Physics, A118:261-301.
3. Brassard, J.R., and M.J. Correia. 1977. "A Computer Program for Fitting Multimodal Probability Density Functions," Computer Programs in Biomedicine 7, p. 1-20.
4. Brown, K. M., and J.E. Dennis, Jr. 1970. "Derivative Free Analogues of the Levenberg-Marquardt and Gauss Algorithms for Nonlinear Least Squares Approximation," Numer. Math., 18:289-297.
5. Chu, Y.Y., and G. Scharff-Goldhaber. 1977. "Decay of Th-234 to the Pa-234 Isomers," Physical Review C, 17(4).
6. Davidson, W. C. 1965. "Variable Metric Method for Minimization," Argonne National Laboratory, ANL-5990 (Rev.).
7. Davidson, W.F., and R.D. Connor. 1968. "The Gamma-Ray Spectrum of Th-227," Nuclear Physics, A116:342-362.
8. Davidson, W.F., and R.D. Connor. 1970. "The Decay of Ra-223 and Its Daughter Products. I: The Decay of Ra-223," Nuclear Physics, A149:363-389.
9. Davidson, W.F., and R.D. Connor. 1970. "The Decay of Ra-223 and Its Daughter Products. II. The Decay of Rn-219 and Po-215," Nuclear Physics, A149:385-391.
10. Fletcher, R. 1970. (FORTRAN Program included as an appendix of Ref. 10) Computer J., 13 (317).

11. Fletcher, R., and M.J.D. Powell. 1963. "A Rapidly Convergent Descent Method for Minimization," *The Computer J.*, 6:163-168.
12. Garbow, B.S. 1969. "Variable Metric Minimization," Argonne National Laboratory, ANL Z013.
13. Godart, J., and A. Gizon. 1973. "Niveaux de Pa-234 Atteints Par La Desintegration De Th-234," *Nuclear Physics*, A127:159-176.
14. Gunnink, R.J.B., et al. 1969. "Gamma-Ray Energies and Intensities," Lawrence Livermore Laboratory, UCID-15439.
15. Heath, R.L. 1975. "Gamma-Ray Spectrum Catalogue Ge(Li) and Si (Li) Spectrometry," Third Edition, Physics TID-4500.
16. Hyde, E.K., J. Perlman, and G.T. Seaborg. 1964. "The Nuclear Properties of the Heavy Elements," Vol. II, Prentice-Hall, Inc., Englewood Cliffs, NJ.
17. Kearn, Jean. 1969. "Computer Analysis of Nuclear Spectra and γ -energy Standards," *Nuclear Instruments and Methods*, 79:233-239.
18. Kogan, R.M., I.M. Nazarov, and S.D. Fridman. 1969. "Gamma Spectrometry of Natural Environments and Formations, Moscow" (in Russian).
19. Kurcewicz, W., et al. 1977. "Precise Energies of Gamma Rays From the Th-230 and Th-228 Decay," *Nuclear Instruments and Methods*, 146:613-614.
20. Lederer, C.M., J.M. Hollander, and J. Perlman. 1968, 1978. "Table of Isotopes," 6th and 7th Editions, John Wiley and Sons, Inc., New York.
21. Lingeman, E.W., et al. 1969. *Nuclear Physics*, 133:630.
22. McNelles, L.A., and J.L. Campbell. 1975. "Analytic Approximations to Peak Shapes Produced by Ge(Li) and Si(Li) Spectrometers," *Nuclear Instruments and Methods*, 127:73-81.

23. Momeni, M.H. 1978. "Competitive Radiation-Induced Carcinogenesis: An Analysis of Data From Beagle Dogs Exposed to Ra-226 and Sr-90," *Health Phys.*, 36:295-310.
24. Op De Beeck, J. 1975. "Gamma-Ray Spectrometry Data Collection and Reduction by Simple Computing Systems," *Atomic Energy Review*, 13(4).
25. Phillips, G.W., and K.W. Marlow. 1976. "Automatic Analysis of Gamma-Ray Spectra From Germanium Detectors," *Nuclear Instruments and Methods*, 137:525-536.
26. Sampson, T.E. 1973. "Precision Measurement of Gamma-Ray Energies From U-238 Daughters, II," *Nuclear Instruments and Methods*, 111:209-211.
27. Smith, A.K., and H.A. Wollenberg. 1972. "High-Resolution Gamma Ray Spectrometry for Laboratory Analysis of the Uranium and Thorium Decay Series," *Natural Radiation Env.*, Vol. 1, US-ERDA.
28. Taylor, H.W. 1973. "Gamma-Ray Emitted by Uranium and Thorium in the Energy Range 10-120 keV," *International Journal of Applied Radiation and Isotopes*, 23:593-597.
29. Teoh, W., R.D. Connor, and R.H. Betts. 1974. "The Decay of U-235," *Nuclear Physics*, A228:432-444.
30. Zobel, V., et al. 1976. "Ra-226 as Calibration Standard for Ge(Li) Spectrometers," *Nuclear Instruments and Methods*, 141:329-336.

APPENDIX A. PREPARATION AND ANALYSIS OF STANDARDS

Standards were prepared by mixing 1 g of the ore into a sand matrix to a total weight of about 10 g. The solutions were pipetted into a 10-g sand matrix, dried, and placed in a two-piece rigid plastic, cylindrical container (4.1 mm in diameter by 1.6 mm high) and covered with a cellulose filter. The samples were packed with a pneumatic press to a height of about 5 mm and then covered with hot wax. Finally, the plastic lid was greased with a high vacuum compound and the sample was sealed. Similar procedures were applied to all samples and blanks, except for those already in a sand matrix, e.g., uranium ore and soil.

Radium Standards

The standards were prepared from a radium-226 solution and clean beach sand according to the procedure described above. Ten grams of sand were mixed with 1 ml of the solution, dried at room temperature, and covered with hot wax. Each standard was then measured by the same technique previously utilized for calibration. The measurements were repeated 50 days after sample preparation.

In addition, two aliquots (each of 25 λ volume) of the same radium solution were heated on two steel disks to evaporate the polonium. The radium was then measured by alpha spectroscopy. The activities of the two samples, measured for a duration of 2000 seconds, were 1344.0 pCi/ml and 1340.7 pCi/ml, with the average of 1342.4 pCi/ml. On the basis of these measurements, the activities of the two radium-226 standards in the sand matrix were determined to be 1355.8 pCi (standard A) and 1342.4 (standard B), with an average of 1349.1 pCi.

Results of the spectrographic analyses of radium standards A and B, for the counting period 1.5×10^5 sec, are shown in Tables A.1 through A.6. The activities of the standards are 1262.8 pCi (A) and 1279.6 pCi, with errors of about 1% from detection of a 186 keV peak of Ra-226. The average activities from detection of Pb-214 peaks are 1226.1 pCi, with a 0.48% error for standard A, and 1357.3 pCi, with a 0.28% error for standard B. The average activities from the detection of Bi-214 peaks are 1234.4 pCi, with a 0.48% error for standard A, and 1360.2 pCi with a 0.39% error. Comparison of standards A and B indicates that the activity of standard B is higher, in contrast to the results of the alpha spectroscopy. However, the difference is small and well within the expected range of the statistical variation. The average of the activities of standards A and B is 1271.2 pCi from Ra-226, 1291.7 pCi from Pb-214, and 1297.3 pCi from Bi-214. The average of all of the measurements is 1286.7 pCi for Ra-226. The difference between the average activity determined by alpha spectroscopy and that determined by gamma spectroscopy is only 4.85%. Since the error of pipetting 25 λ is larger than that of pipetting 1 ml, the difference could be largely due to sample preparation. Thus, the activity of the solution is the average of the activities determined by gamma spectroscopy.

Pitchblende Ore Standard No. 6*

A sample of the ore was dried to a constant weight. Then 0.502 g of the ore was mixed with 23.451 g of clean beach sand with low specific activity and the mixture divided into two samples, 6A (11.964 g) and 6B (11.929 g). The ore made up only 2.096% of the sample. The activities of the samples were calculated on the basis of the natural abundance of the U-238 isotope (99.28%), the decay coefficient λ (1.537×10^{-10} /year) and the ratio U_3/U_3O_8 (0.849). The control sample was prepared with 12.0 g of beach sand. The U-238 activities of the samples were:

6A	3.7715×10^4 pCi
6B	3.7605×10^4 pCi
Control	3.50 pCi

*U.S. Atomic Energy Commission, New Brunswick Laboratory. The sample (dried at 110° C) contained 53.55% U_3O_8 .

Since the samples were prepared in 1978, the activity had reached secular radioactive equilibrium with respect to Po-218, Pb-214, and Bi-214 (radon daughters).

The results of gamma spectroscopic analysis of this sample are shown in Table A.7. The mean activities and the detection limits are given in Tables A.8 and A.9. The mean activity of the members of the U-238 series is about 3.77×10^4 pCi, with the lowest error (0.16%) for Pb-214 and the highest (13.69%) for U-234. This activity is in good agreement with the activity of the standards. The activity of the members of the actinium series is about 1.77×10^3 pCi with the lowest error (1.34%) for Ra-223 and the highest (14.54%) for Pa-231. The ratio of the specific activity of U-238 to that of U-235 is 21.299, in good agreement with the ratio of 21.348 calculated from the natural abundances of these two nuclides. The activity of the thorium series in the ore sample was not detectable (Table A.9).

Pitchblende Ore Standard No. 100*

The activities of selected radionuclides in this reference material have been carefully and extensively measured (Sill and Willis 1965; Sill and Williams 1969; Sill and Hindman 1974; Sill 1976). These measurements indicated that the sample was in secular radioactive equilibrium with the recommended activity for the uranium series $6.06 \pm 0.04 \times 10^3$ disintegrations per minute per gram (dpm/g) and for the actinium series $2.82 \pm 0.09 \times 10^2$ (dpm/g).

The Percival and Martin (1974) analysis of the same ore sample produced the activities (at a 95% confidence level) for members of each series. 1.8873 g of the ore was mixed with beach sand to a total weight of 12 g. The results of this analysis are in Tables A.10, A.11, and A.12.

The mean activity of Pa-234m is 5.587×10^3 pCi with an error of 3.20% (Table A.11). The activities for the individual lines and the errors of the

*Made available by Claude Sill, Health Services Laboratory, U.S. Energy Research and Development Administration, Idaho Falls, Idaho.

measurements of Pa-234m are 5.603×10^3 pCi (4.95%) at 742.8 keV and 5.576×10^3 pCi (4.20%) at 766.4 keV. The lines at 258.4 keV and 1001.1 keV interfere with the activity of Pb-214 and Bi-214, respectively. The activities from these lines have been incorporated into the mean value, even though they are not listed here. The activity of Pa-234m is a measure of U-238 activity under secular radioactive equilibrium. The activity of the other nuclide in U-238, Pa-234, could not be determined (Table A.12) since the line at 946.0 keV (a major line) was not statistically observable. The previously reported activity for this ore is $6.06 \pm 0.04 \times 10^3$ dpm/g, corresponding to 5.158×10^3 pCi (Sill 1977; Percival and Martin 1974).

The activity of U-234, calculated from the 53.1 keV line (Table A.10), is 9.837×10^3 pCi (14.73%). However, this line has interference from Pb-214, but since the mean activity of Pb-214, 5.337×10^3 pCi (3.61%), has been used for correction of the interference, the activity for U-234 (Table A.11) is a reasonable estimate for the nuclide. This calculated activity suggests that the ore sample is not in secular radioactive equilibrium with respect to U-238 and U-234.

Thorium-230 activity was determined (Table A.10) from the 67.6 keV and the 143.8 keV lines to be 4.788×10^3 pCi (9.7%). The mean Th-230 activity is shown in Table A.11. The 143.8 keV line has interference from Ra-223 and U-235. But since the activity of either Pa-234m or U-234 is used for correction of the interference, the calculated Th-230 activity is a reasonable estimate. This result suggests a lack of equilibrium between U-234 and Th-230.

The mean activities of Ra-226, Bi-214, and Pb-214 (Table A.11) are 6.063×10^3 pCi (2.59%), 5.316×10^3 pCi (0.2%), and 5.337×10^3 pCi (3.61%) respectively. The mean activities of Bi-214 and Pb-214 are in good agreement, but the activity of Ra-226 is 7% higher than the mean activities of the two radon (Rn-222) daughters. Since the only usable line for Ra-226 is 186.0 keV (Table A.10), and this line is in interference with U-235 activity at 185.7 keV, the 7% may be introduced from the U-235 correction. The mean U-235 activity (Table A.11) is 1.875×10^2 pCi (6.55%). If the ratio of the activity of U-235 to that of U-238 is proportional to the ratio of the natural abundance of U-235 to that

of U-238, then, on the basis of the Pa-234m activity, that of U-235 should be 2.617×10^2 pCi. The activity of U-235 was determined from the following lines: 114.4 keV [1.301×10^2 pCi (10.55%)], 139.8 keV [1.873×10^3 pCi (12.90%)], 163.3 keV [3.785×10^2 pCi (7.6%)], 194.9 keV [6.836×10^2 pCi (15.35%)], and two lines at 143.8 keV and 241.9 keV, both complicated by interference. The mean U-235 activity is 1.875×10^2 pCi (6.55%) (Table A.11), with a range of 1.3×10^2 to 6.84×10^2 pCi. Thus, the 7% difference between the Ra-226 activity and those of Bi-214 and Pb-214 is not significant, and a better estimate for the Ra-226 activity is the average of the mean activities for Bi-214 and Pb-214, 5.327×10^3 pCi, which is in agreement with those reported by Percival and Martin (1974) and Sill et al. (1977).

The activity of Pb-210 [5.928×10^3 pCi (1.10%)] is 10% larger than the radon daughter activities. This difference seems to be significant and needs further evaluation. The mean activities of the U-235 daughters (Table A.11) are 2.401×10^2 pCi (1.52%) for Rn-219, 2.249×10^2 pCi (1.82%) for Th-227, 2.367×10^2 pCi (1.53%) for Ra-223, and 2.116×10^2 pCi (27.5%) for Pa-231.

The activity of Pa-234m, estimated from the average activity of the actinium series, is 4.88×10^3 pCi, which is smaller than the mean activity of Pa-234m shown in Table A.11, 5.587×10^3 pCi. The activity of Th-234 is 5.428×10^3 pCi (1.30%), which is in agreement with the Pa-234m activities measured directly from the spectrum. Thus, the differences between U-238, U-234, and U-235 may not be an artifact and, although small, (about 10%) may be a real observation.

Table A.1. Gamma Spectrographic Analysis of Radium Standard A
RA STANDARD A COMPLETE EQUILIBRIUM

COUNT TIME (SEC): 1.50000E 05

ENERGY CALIBRATION

ID: NOV. 17/80 OFF=80 GAIN=100/F6

EFFICIENCY CALIBRATION 1

ID: NOV. 12/80 OFF=80 G=100/F6 E=155/610/2000

EFFIC. CORRECTED COUNT RATE

REGION: 1 TO 4000

PK. NO.	CENTR. CHAN.	CENTR. KEV	ERROR CHAN.	FWHM KEV	AREA COUNTS	CNT. RATE CNTS/SEC	ERROR % AREA	C
1	16.5	29.99	1.73	1.42	806	1.1688E-01	42.85	1
2	37.9	35.86	0.01	1.23	777074	9.0255E-01	0.35	1
3	75.7	46.48	0.10	1.26	6446	5.6894E-01	4.00	
4	98.8	53.09	0.07	1.21	5142	4.0245E-01	2.90	
5	173.2	74.90	0.04	1.26	47116	2.9024E-00	1.30 *	
6	181.1	77.26	0.02	1.26	83187	5.0457E-00	0.85 *	
7	189.0	79.63	0.21	1.26	5312	3.1773E-01	8.20 *	
8	204.1	84.16	0.15	1.37	3279	1.9180E-01	9.75 *	
9	215.8	87.68	0.03	1.37	28141	1.623/E 00	1.50 *	
10	224.9	90.43	0.05	1.37	10495	6.0045E-01	2.70 *	
11	234.6	93.34	0.33	1.37	1271	7.2210E-02	13.55 *	
12	557.0	186.35	0.03	1.32	23254	2.0866E-00	1.00	
13	749.0	242.21	0.03	1.28	30683	3.4697E-00	1.05	
14	806.9	259.04	0.11	1.26	1779	2.1521E-01	4.95	
15	861.2	274.83	0.17	1.50	1245	1.6022E-01	7.80	
16	932.1	295.47	0.01	1.33	64061	8.9183E-00	0.55	
17	1127.2	352.24	0.01	1.36	101104	1.7173E-01	0.50	
18	1246.5	386.97	0.25	1.25	544	1.0283E-01	12.55	
19	1254.2	389.21	0.21	1.25	862	1.6401E-01	9.55	
20	1480.8	455.15	0.39	1.68	490	1.1036E-01	17.90	
21	1504.3	462.02	0.49	1.19	279	6.3807E-02	24.35	
22	1508.9	463.36	0.59	1.19	218	5.0004E-02	25.60	
23	1532.3	470.17	0.50	1.18	263	6.1222E-02	24.10	
24	1569.4	480.97	0.27	1.27	630	1.5003E-01	11.85	
25	1591.7	487.47	0.28	1.61	677	1.6339E-01	12.00	

Table A.1. (cont'd)

26	1673.1	511.15	0.44	1.78	1082	2.7370E-01	9.35	1
27	1752.3	534.23	0.41	1.52	387	1.0233E-01	16.60	
28	1911.8	580.68	0.29	1.15	404	1.1715E-01	14.30	
29	2012.1	609.88	0.01	1.51	62088	1.9247E 01	0.60	
30	2205.0	666.08	0.11	1.51	1669	5.5188E-01	4.25	
31	2334.9	703.93	0.26	1.40	427	1.4825E-01	10.75	
32	2391.9	720.53	0.42	1.88	379	1.3444E-01	13.85	
33	2470.0	743.28	0.23	1.36	409	1.4940E-01	10.55	
34	2558.8	769.15	0.06	1.63	5131	1.9377E 00	1.80	
35	2618.9	786.64	0.13	1.65	1273	4.9168E-01	4.45	
36	2688.6	806.95	0.11	1.65	1271	5.0385E-01	4.20	
37	2801.6	839.86	0.22	1.46	670	2.7696E-01	9.25	
38	3128.0	934.95	0.08	1.65	2574	1.1978E 00	2.75	
39	3231.2	965.00	0.32	1.06	260	1.2546E-01	19.05	
40	3533.7	1053.10	0.57	1.69	220	1.1745E-01	18.40	
41	3768.0	1121.29	0.03	1.77	11400	6.5360E 00	0.85	
42	3887.8	1156.17	0.12	1.60	1184	7.0191E-01	4.20	
43	3950.3	1174.36	1.96	1.15	210	1.2656E-01	70.30	1
44	3965.1	1178.68	0.01	1.15	776315	4.6968E 02	0.45	1

ISOTOPE ANALYSIS

UNITS : PCI/

CONVERSION FACTOR : 1.0000E 06

SIZE : 1.0000E 00

PEAK ANALYSIS

PK	CENT	NUCLIDE	TYPE	GAMMA KEV	ACTIVITY	% ERROR
1	29.9					
2	35.8					
3	46.4	PB 210		46.5	4.6358E 02	
4	53.0	PB 214		53.1		4.00

Table A.1. (cont'd)

5	74.9				
6	77.2				
7	79.6				
8	84.1				
9	87.6				
10	90.4				
11	93.3				
12	186.3	RA 226	186.0	1.2628E 03	1.00
13	242.2	PB 214	241.9	1.2249E 03	1.05
14	259.0	PB 214	259.1	2.7744E 03	4.95
15	274.8	BI 214	274.5		
		PB 214	274.8		
16	295.4	PB 214	295.2	1.2235E 03	0.55
17	352.2	PB 214	351.9		
		BI 211	2 351.9	0E 00	0
18	386.9	BI 214	386.8	1.1446E 03	12.55
19	389.2	BI 214	388.9	1.3371E 03	9.55
20	455.1	BI 214	454.9	1.3272E 03	17.90
21	462.0	PB 214	462.2	9.2306E 02	24.35
22	463.3				
23	470.1				
24	480.9				
25	487.4				
26	511.1				
27	534.2				
28	580.6	PB 214	580.3	9.9550E 02	14.30
29	609.8	BI 214	609.5	1.2327E 03	0.60
30	666.0	BI 214	665.6	1.2579E 03	4.25
31	703.9				
32	720.5				
33	743.2				
34	769.1	BI 214	768.5	1.1410E 03	1.80
35	786.6				
36	806.9	BI 214	806.2	1.3080E 03	4.20
37	839.8	BI 214	839.1	1.1426E 03	9.25
38	934.9				
39	965.0	BI 214	964.1	1.0486E 03	19.05
40	1053.1				
41	1121.2	BI 214	1120.2	1.2631E 03	0.85
42	1156.1	BI 214	1155.1	1.1844E 03	4.20
43	1174.3				
44	1178.6				

Table A.2. Mean Activities of Nuclides in Radium Standard A

MEAN ACTIVITIES

NUCLIDE	TYPE	ACTIVITY	% ERROR	% CHISQ	HALF[MIN]
RA 226		1.2628E 03	1.00	0	8.40E 08
PB 210		4.6358E 02	4.00	0	1.17E 07
BI 211	2	0E 00	0	0	2.15E 00
PB 214		1.2261E 03	0.48	2.78	2.67E 01
BI 214		1.2344E 03	0.46	0.84	1.97E 01

Table A.3. Detection Limits of Nuclides in Radium Standard A

DETECTION LIMITS

NUCLIDE	TYPE	GAMMA	ACTIVITY	% ERROR
AC 227		85.6	2.0070E 04	
TH 228		215.9	4.0991E 02	
RA 224		241.0	1.8082E 03	
PB 212		238.6	3.2486E 00	
TH 231		108.4	5.6787E 01	
TI 210		1110.0	1.9561E 03	
PO 214		799.5	5.6526E 03	
FR 223		234.0	2.9062E 03	
PB 211		65.4	3.6726E 01	
RN 219		271.2	1.1360E 01	
TH 234		63.3	5.7983E 01	
PA 234		946.0	5.4813E 03	
TH 230		67.7	3.3480E 02	
U 235		143.8	1.1040E 01	
TH 227		235.9	8.9203E 00	
RA 223		269.4	1.0016E 01	
PA 231		302.5	8.4109E 01	
PA 234M		1001.0	3.1494E 02	
AC 228		583.2	1.0925E 01	
TI 208		860.6	7.3245E 01	
BI 212		473.5	1.1683E 01	

Table A.4. Gamma Spectrographic Analysis of Radium Standard B

RADIUM 226 STANDARD B EQUILIBRIUM

COUNT TIME (SEC): 1.50000E 05

ENERGY CALIBRATION

ID: NOV. 17/80 OFF=80 GAIN=100/F6

EFFICIENCY CALIBRATION 1

ID: NOV. 12/80 OFF=80 G=100/F6 E=155/610/2000

EFFIC. CORRECTED COUNT RATE

REGION: 1 TO 4000

PK. NO.	CENTR. CHAN.	CENTR. KEV	ERROR CHAN.,	FWHM KEV	AREA COUNTS	CNT. RATE CNTS/SEC	ERRUR % AREA	C
1	22.2	31.53	0.02	0.50	1331	1.8082E-01	58.20	
2	42.6	37.16	0.01	1.17	777869	8.6740E 01	0.30	1
3	75.5	46.42	0.09	1.25	6952	6.1432E-01	3.25	
4	98.9	53.12	0.11	1.21	5723	4.4772E-01	4.10	
5	124.4	60.51	0.67	1.45	851	6.0023E-02	25.95	
6	173.2	74.92	0.03	1.30	51985	3.2020E 00	1.10	1
7	181.1	77.25	0.02	1.30	90606	5.4960E 00	0.85	1
8	188.7	79.55	0.13	1.30	6698	4.0081E-01	5.60	1
9	204.1	84.14	0.43	1.30	1551	9.1316E-02	20.85	1
10	215.9	87.71	0.04	1.30	28863	1.6652E 00	1.65	1
11	225.0	90.44	0.07	1.30	10544	6.0324E-01	3.20	1
12	556.9	186.33	0.02	1.28	23563	2.1141E 00	1.05	
13	749.0	242.20	0.03	1.28	33604	3.7999E 00	0.90	
14	807.0	259.07	0.14	1.49	2352	2.8456E-01	5.95	
15	861.6	274.95	0.24	1.41	1370	1.7639E-01	9.35	
16	932.1	295.47	0.01	1.34	71126	9.9017E 00	0.30	
17	1127.1	352.22	0.01	1.37	112438	1.9097E 01	0.45	
18	1247.5	387.24	1.21	1.70	632	1.1956E-01	28.40	1
19	1480.9	455.21	0.24	1.73	664	1.4956E-01	12.30	
20	1505.1	462.23	0.52	1.75	394	9.0150E-02	15.70	
21	1569.3	480.95	0.23	1.53	825	1.9646E-01	10.70	
22	1591.8	487.49	0.25	1.68	844	2.0370E-01	10.35	

Table A.4. (cont'd)

23	1673.9	511.38	0.49	1.78	951	2.4067E-01	9.95
24	1751.5	533.99	0.32	1.00	275	7.2685E-02	24.60
25	1911.4	580.57	0.27	1.29	498	1.4437E-01	14.35
26	2012.0	609.87	0.01	1.51	684/1	2.1228E 01	0.45
27	2204.9	666.06	0.09	1.52	1731	5.7237E-01	3.75
28	2334.2	703.71	0.28	1.50	538	1.8674E-01	11.60
29	2392.0	720.54	0.29	1.55	409	1.4508E-01	13.40
30	2469.7	743.17	0.34	1.93	467	1.7056E-01	9.20
31	2558.7	769.11	0.07	1.55	5675	2.1430E 00	2.25
32	2618.9	786.64	0.13	1.65	1327	5.1253E-01	5.25
33	2688.8	807.01	0.11	1.62	1391	5.5146E-01	4.05
34	2756.5	826.73	0.68	1.04	130	5.2851E-02	36.65
35	2801.5	839.85	0.16	1.57	869	3.5923E-01	6.20
36	3128.0	934.93	0.08	1.77	2969	1.3816E 00	2.35
37	3230.7	964.85	0.44	1.76	382	1.8429E-01	15.30
38	3595.7	1071.13	0.36	1.11	178	9.6907E-02	18.85
39	3767.9	1121.29	0.04	1.75	12386	7.1013E 00	0.95
40	3887.7	1156.15	0.11	1.90	1488	8.8212E-01	3.50
41	3949.9	1174.24	1.25	1.16	227	1.3679E-01	52.65
42	3968.9	1179.77	0.01	1.16	778678	4.7156E 02	0.45

ISOTOPE ANALYSIS

UNITS : PCI/

CONVERSION FACTOR : 1.0000E 05

SIZE : 1.0000E 00

PEAK ANALYSIS

PK	CENT	NUCLIDE	TYPE	GAMMA KEV	ACTIVITY	DECAY CORR	% ERROR
1	31.5						
2	37.1						
3	46.4	PB 210		46.5	4.9997E 02	5.0001E 02	3.25
4	53.1	PB 214		53.1			
5	60.5						
6	74.9						
7	77.2						
8	79.5						
9	84.1						
10	87.7						
11	90.4						
12	186.3	RA 226		186.0	1.2796E 03	1.2796E 03	1.05
13	242.2	PB 214		241.9	1.3415E 03	8.7058E 04	0.90
14	259.0	PB 214		259.1	3.6680E 03	2.3806E 05	5.95
15	274.9	BI 214		274.5			
		PB 214		274.8			

Table A.4. (cont'd)

16	295.4	PB 214	295.2	1.3584E 03	8.8165E 04	0.30
17	352.2	PB 214	351.9			
		BI 214	351.9	0E 00	0E 00	0
18	387.2	BI 214	386.8	1.3297E 03	1.1697E 05	28.40
19	455.2	BI 214	454.9	1.7985E 03	1.5820E 05	12.30
20	462.2	PB 214	462.2	1.3035E 03	8.4601E 04	15.70
21	480.9					
22	487.4					
23	511.3					
24	533.9					
25	580.5	PB 214	580.3	1.2271E 03	7.9842E 04	14.35
26	609.8	BI 214	609.5	1.3594E 03	1.1958E 05	0.45
27	666.0	BI 214	665.8	1.3045E 03	1.1476E 05	3.75
28	703.7					
29	720.5					
30	743.1					
31	769.1	BI 214	768.5	1.2620E 03	1.1100E 05	2.25
32	786.6					
33	807.0	BI 214	806.2	1.4315E 03	1.2592E 05	4.05
34	826.7					
35	839.8	BI 214	839.1	1.4819E 03	1.3035E 05	6.20
36	934.9					
37	964.8	BI 214	964.1	1.5407E 03	1.3552E 05	15.30
38	1071.1					
39	1121.2	BI 214	1120.2	1.3723E 03	1.2021E 05	0.95
40	1156.1	BI 214	1155.1	1.4886E 03	1.3094E 05	3.50
41	1174.2					
42	1179.7					

Table A.5. Mean Activities of Nuclides in Radium Standard B

MEAN ACTIVITIES

NUCLIDE	TYPE	ACTIVITY	% ERROR	% CH150	HALFLIFE
RA 226		1.2796E 03	1.05	0	8.40E 03
MB 210		4.9997E 02	3.25	0	1.17E 07
BI 211	2	0E 00	0	0	2.15E 00
PB 214		1.3573E 03	0.28	1.52	2.67E 01
BI 214		1.3602E 03	0.39	0.69	1.97E 01

Table A.6. Detection Limits of Nuclides in Radium Standard B

DETECTION LIMITS

NUCLIDE	TYPE	GAMMA	ACTIVITY	% ERROR
AC 227		85.6	2.2347E 04	
TH 228		215.9	5.3194E 02	
RA 224		241.0	1.9657E 03	
PB 212		238.6	4.0372E 00	
IH 231		108.4	6.1511E 01	
TI 210		1110.0	1.6973E 03	
PO 214		799.5	5.6375E 03	
FR 223		234.0	2.4507E 03	
PB 211		65.4	2.9596E 01	
RW 219		271.2	1.2235E 01	
TH 234		63.3	4.1996E 01	
PA 234		946.0	6.4643E 03	
IH 230		67.7	3.9545E 02	
U 235		143.8	1.2859E 01	
TH 227		235.9	9.4196E 00	
RA 223		269.4	9.9645E 00	
PA 231		302.5	1.0159E 02	
PA 234M		1001.0	3.6008E 02	
AC 228		583.2	1.0993E 01	
TI 208		860.6	5.3944E 01	
BI 212		473.5	1.4063E 01	

Table A.7. Gamma Spectrographic Analysis of the Pitchblende
Ore Standard No. 6

ISOTOPE ANALYSIS

UNITS : PCI/

CONVERSION FACTOR : 1.0000E 06

SIZE : 1.0000E 00

PEAK ANALYSIS

PK	CENT KEV	NUCLIDE	TYPE	GAMMA KEV	ACTIVITY	% ERROR
1	46.6	PB 210		46.5	3.8421E 04	1.55
2	50.1					
3	53.3	PB 214		53.1		
		U 234	2	53.2	3.7702E 04	13.69
4	63.3	TH 234		63.3	3.6528E 04	0.95
5	67.7	TH 230		67.7	3.7139E 04	2.55
6	93.4					
7	95.7					
8	98.5					
9	99.5					
10	100.2					
11	103.9					
12	106.8					
13	110.6					
14	112.6	TH 227		113.1	1.7668E 03	3.55
15	114.5	U 235		115.2	1.6604E 03	5.20
16	116.4	TH 227		116.5	1.6200E 03	10.50
17	124.2					
18	132.2					
19	144.0	RA 223		144.2		
		U 235		143.8		
		TH 230		144.2		
20	154.3	RA 223		154.3	1.8230E 03	3.70
21	158.6	RA 223		158.4	1.8686E 03	11.75
22	163.4	U 235		163.3	1.7670E 03	4.20
23	163.4					
24	183.7					
25	184.5					
26	186.1	U 235		185.7		
		RA 226	2	186.0	3.6568E 04	8.95
27	195.9	U 235		194.9	4.4636E 03	10.55
28	202.1	U 235		202.1	1.7666E 03	13.50
29	205.4					
30	205.4					

Table A.7. (cont'd)

31	210.7	TH 227	210.7	1.8970E 03	11.25
32	236.1	TH 227	235.9	1.7620E 03	2.20
33	242.1	PB 214	241.9	3.7855E 04	0.20
34	256.3	TH 227	256.2	1.7742E 03	3.10
35	258.7	PA 234M	258.4	3.7715E 04	5.45
36	259.2	PB 214	259.1	3.7715E 04	16.95
37	269.5	RA 223	269.4	1.7031E 03	1.55
38	271.3	RN 219	271.2	1.6749E 03	1.50
39	273.5				
40	274.9	BI 214	274.5		
		PB 214	274.8		
41	283.8	PA 231	283.6	1.7977E 03	22.20
42	286.3	TH 227	286.1	1.7808E 03	12.75
43	295.3	PB 214	295.2	3.7633E 04	0.30
44	300.0	PA 231	299.9		
		TH 227	299.9		
45	302.9	PA 231	302.5	1.7659E 03	19.25
46	314.5	TH 227	314.8	1.9667E 03	10.50
47	324.0	RA 223	323.8	1.9402E 03	4.50
48	330.0	TH 227	329.9	1.7681E 03	5.75
49	334.1	RA 223	333.8		
		TH 227	334.0		
50	338.3	BI 214	338.3		
		RA 223	338.3		
51	338.3				
52	352.0	PB 214	351.9		
		BI 211	2	351.9	
53	386.9	BI 214	386.8	3.7680E 04	3.70
54	389.0	BI 214	388.9	3.9566E 04	2.65
55	401.9	RN 219	401.8	1.7623E 03	3.35
56	404.7				
57	405.5	BI 214	405.7	3.7869E 04	10.80
58	427.3				
59	445.0	RA 223	445.0	1.7619E 03	16.05
60	455.0	BI 214	454.9	3.7718E 04	5.55
61	462.0	PB 214	462.2	3.7475E 04	5.20
62	470.0				
63	474.7	BI 214	474.6	2.1567E 04	102.35
64	480.6				
65	482.2				
66	486.9				
67	487.6				
68	510.2				
69	517.0				
70	518.2				
71	533.8				
72	543.5				
73	572.8				
74	580.3	PB 214	580.3	3.7716E 04	3.15
75	609.5	BI 214	609.5	3.7504E 04	0.35
76	616.3				
77	638.5				

Table A.7. (cont'd)

78	639.9				
79	649.6				
80	665.6	BI 214	665.6	3.6863E 04	48.55
81	668.1				
82	668.1				
83	681.7				
84	690.0				
85	690.7				
86	691.5				
87	703.3				
88	720.0				
89	732.2				
90	742.8	PA 234M	742.8	3.7718E 04	4.15
91	753.1				
92	768.6	BI 214	768.5	3.7721E 04	2.15
93	786.1				
94	806.4	BI 214	806.2	3.7603E 04	1.35
95	821.5				
96	826.3				
97	832.2				
98	839.3	BI 214	839.1	3.7923E 04	1.75
99	847.1				
100	904.6				
101	934.3				
102	964.4	BI 214	964.1	3.7686E 04	3.75
103	986.6				
104	987.8				
105	1001.3	PA 234M	1001.0	3.7715E 04	1.70
106	1052.2				
107	1070.3				
108	1096.8				
109	1102.5				
110	1110.4				
111	1120.5	BI 214	1120.2	3.7834E 04	0.30
112	1133.9	BI 214	1133.8	3.7775E 04	7.35
113	1155.4	BI 214	1155.1	3.7839E 04	1.35
114	1177.7				
115	1182.3				

Table A.8. Mean Activities of Nuclides in
Pitchblende Ore Standard No. 6

MEAN ACTIVITIES

NUCLIDE	TYPE	ACTIVITY	% ERROR	% CHISQ
U 234	2	3.7702E 04	13.69	0
RA 226	2	3.6568E 04	8.95	0
PB 210		3.8421E 04	1.55	0
RW 219		1.6883E 03	1.36	1.86
BI 211				
TH 234		3.6528E 04	0.95	0
TH 230		3.7139E 04	2.55	0
PB 214		3.7785E 04	0.16	0.13
U 235		1.7606E 03	3.09	10.44
TH 227		1.7683E 03	1.48	0.81
RA 223		1.7370E 03	1.34	2.03
BI 214		3.7709E 04	0.21	0.16
PA 231		1.7793E 03	14.54	0.88
PA 234M		3.7716E 04	1.51	0.00

Table A.9. Detection Limits of Nuclides in
Pitchblende Ore Standard No. 6

DETECTION LIMITS

NUCLIDE	TYPE	GAMMA	ACTIVITY
AC 227		160.0	1.1408E 05
TH 228		217.0	3.3133E 03
RA 224		240.9	7.2667E 04
PB 212		238.6	2.5422E 01
BI 212		1078.8	3.8601E 03
TH 231		58.5	3.8462E 03
TI 210		789.2	4.9170E 04
PO 214		799.5	5.5953E 04
FR 223		234.0	7.3529E 04
PB 211		65.4	1.8301E 03
PA 234		946.0	5.3890E 04

Table A.10. Gamma Spectrographic Analysis of Pitchblende
Ore Standard No. 100

SAMPLE ORE SILL DECEMBER 4, 1980

COUNT TIME (SEC): 3.30000E 05

ENERGY CALIBRATION
ID: NOV. 17/80 OFF=80 GAIN=100/F6

ISOTOPE ANALYSIS
UNITS : PCI/
CONVERSION FACTOR : 1.0000E 06
SIZE : 1.0000E 00

PEAK ANALYSIS

PK	CENT KEV	NUCLIDE	TYPE	GAMMA KEV	ACTIVITY	% ERROR
1	46.5	PB 210		46.5	5.9284E 03	1.10
2	49.9					
3	53.1	PB 214		53.1		
		U 234	2	53.2	9.8365E 03	14.73
4	63.1	TH 234		63.3	5.4280E 03	1.30
5	67.1					
6	67.6	TH 230		67.7	4.7884E 03	9.70
7	114.4	U 235		115.2	1.3008E 02	10.55
8	123.7					
9	130.6	RN 219		130.8	4.5691E 02	14.90
10	139.8	U 235		140.8	1.8730E 03	12.90
11	143.8	RA 223		144.2		
		U 235		143.8		
		TH 230		144.2		
12	154.1	BI 212	2	154.0	1.8976E 02	43.43
		RA 223		154.3		
13	163.3	U 235		163.3	3.7853E 02	7.60
14	165.5					
15	185.9	U 235		185.7		
		RA 226	2	186.0	6.0630E 03	2.59
16	195.8	U 235		194.9	6.8355E 02	15.35
17	205.2					
18	210.4	TH 227		210.7	2.3990E 02	14.70
19	235.9	TH 227		235.9	2.2467E 02	2.15
20	241.9	U 235		240.9		
		PB 214		241.9		
		RA 224	2	241.0	4.9465E 01	635.33
21	256.1	TH 227		256.2	2.3784E 02	4.10

Table A.10. (cont'd)

22	258.7	PA 234H	258.4			
		PB 214	259.1			
23	260.1					
24	269.3	RA 223	269.4	2.3477E 02	1.60	
25	271.1	RN 219	271.2	2.3885E 02	1.60	
26	273.5					
27	274.7	BI 214	274.5			
		PB 214	274.8			
28	283.6	PA 231	283.6	2.1160E 02	27.50	
29	286.1	TH 227	286.1	2.4728E 02	21.25	
30	295.1	BI 212	2	295.1	0E 00	0
		PB 214	295.2			
31	299.9	PA 231	299.9			
		TH 227	299.9			
32	314.3	TH 227	314.8	2.8332E 02	16.05	
33	323.8	RA 223	323.8	2.5825E 02	5.85	
34	329.8	TH 227	329.9	1.8601E 02	8.05	
35	338.0	BI 214	338.3			
		RA 223	338.3			
36	338.6					
37	351.8	PB 214	351.9			
		BI 211	2	351.9	0E 00	0
38	362.4					
39	386.7	BI 214	386.8	5.5719E 03	3.65	
40	388.8	BI 214	388.9	5.5252E 03	3.65	
41	401.7	RN 219	401.8	2.4611E 02	5.15	
42	404.8					
43	405.6	BI 214	405.7	2.7985E 03	29.55	
44	427.1					
45	444.9	RA 223	445.0	3.4134E 02	14.55	
46	454.7	BI 214	454.9	5.2782E 03	14.80	
47	461.7	PB 214	462.2	5.5537E 03	6.50	
48	469.6					
49	474.3	BI 212	2	473.5	0E 00	0
		BI 214	474.6			
50	480.3					
51	487.0					
52	510.1					
53	511.8					
54	533.6					
55	543.1					
56	572.7					
57	580.1	PB 214	580.3	5.2508E 03	4.35	
58	595.8					
59	609.2	BI 214	609.5	5.3223E 03	0.25	

Table A.10. (cont'd)

60	665.4	BI 214	665.6	5.3320E 03	1.45
61	683.1				
62	703.1				
63	708.0				
64	719.8				
65	742.5	PA 234H	742.8	5.6025E 03	4.95
66	752.7				
67	766.2	PA 234H	766.4	5.5756E 03	4.20
68	768.3	BI 214	768.5	4.9228E 03	0.95
69	785.9				
70	806.1	BI 214	806.2	5.3653E 03	1.95
71	821.2				
72	826.2				
73	832.0				
74	839.1	BI 214	839.1	5.2099E 03	2.85
75	846.8				
76	934.1				
77	964.1	BI 214	964.1	5.6502E 03	4.20
78	1001.1	PA 234H	1001.0		
		BI 214	1000.0		
79	1051.9				
80	1070.0				
81	1096.5				
82	1103.9				
83	1120.2	BI 214	1120.2	5.3665E 03	0.40
84	1133.7	BI 214	1133.8	5.0539E 03	7.45
85	1155.1	BI 214	1155.1	5.4549E 03	1.40
86	1173.0				
87	1177.9				
88	1181.0				
89	1182.3				

Table A.11. Mean Activities of Nuclides in
Pitchblende Ore Standard No. 100

MEAN ACTIVITIES

NUCLIDE	TYPE	ACTIVITY	% ERROR	% CHISQ
U 234	2.	9.8365E 03	14.73	0
RA 226	2	6.0630E 03	2.59	0
PB 210		5.9284E 03	1.10	0
RA 224	2	4.9465E 01	635.33	0
RN 219		2.4009E 02	1.52	3.49
BI 211	2	0E 00	0	0
TH 234		5.4280E 03	1.30	0
TH 230		4.7884E 03	9.70	0
PB 214		5.3374E 03	3.61	2.56
U 235		1.8749E 02	6.55	43.56
TH 227		2.2492E 02	1.82	2.64
RA 223		2.3670E 02	1.53	2.81
BI 214		5.3164E 03	0.20	0.56
PA 231		2.1160E 02	27.50	0
PA 234M		5.5868E 03	3.20	0.23
BI 212	2	3.0246E-01	1087.88	1769.73

Table A.12. Detection Limits of Nuclides in
Pitchblende Ore Standard No. 100

DETECTION LIMITS

NUCLIDE	TYPE	GAMMA	ACTIVITY	% ERROR
AC 227		160.0	1.9260E 04	
TH 228		215.9	6.5498E 02	
PB 212		238.6	4.5991E 00	
TH 231		58.5	5.6317E 02	
TI 210		1110.0	2.2354E 03	
PO 214		799.5	7.8717E 03	
FR 223		234.0	2.3973E 04	
PB 211		65.4	5.2409E 01	
PA 234		946.0	1.2356E 04	
AC 228		583.2	9.5373E 00	
TI 208		860.6	8.7964E 01	

REFERENCES FOR APPENDIX A

1. Percival, D.R. and Martin, D.B. 1974. "Sequential Determination of Radium-226, Radium-228, Actinium-227, and Thorium Isotopes in Environmental and Process Waste Samples," Anal. Chem. 46:1742.
2. Sill, C.W. and Willis, C.P. 1965. "Radiochemical Determination of Lead-210 in Mill Products and Biological Materials," Anal. Chem. 37:1661.
3. Sill, C.W. and Williams, R.L. 1969. "Radiochemical Determination of Uranium and the Transuranium Elements in Process Solutions and Environmental Samples," Anal. Chem. 41:1624.
4. Sill, C.W. and Hindman, F.D. 1974. "Simultaneous Determination of Alpha-Emitting Nuclides of Radium through Californium in Soil," Anal. Chem. 46:1725.
5. Sill, C.W. 1976. "Determination of Thorium and Uranium Isotopes in Ores and Mill Tailings by Alpha Spectrometry," Health Services Laboratory, U.S. Energy Research and Development Administration, Idaho Falls, Idaho.
6. Sill, C.W. 1977. "Simultaneous Determination of ^{238}U , ^{234}U , ^{230}Th , ^{226}Ra , and ^{210}Pb in Uranium Ores, Dusts, and Mill Tailings," Workshop on Methods for Measuring Radiation in and around Uranium Mills, Program Report 3(9), Atomic Industrial Forum, Inc. Washington, D.C.

APPENDIX B. POLYNOMIAL COEFFICIENTS FOR THE EFFICIENCY FUNCTION
AND STATISTICS OF LEAST-SQUARES FIT OF DATA

REGION 1 (40-145 keV)

Number of iterations = 1

Standard deviation of point of unit weight = 0.00257348440848

R-square (goodness-of-fit statistic) = 0.974415106629

<u>i</u>	Parameter A _i	Std. Dev. A _i
1	-0.0627222839251	0.02144994537
2	0.00425700978636	7.399956887E-4
3	-3.104655584E-5	7.823006845E-6
4	6.447985728E-8	2.595272286E-8

REGION 2 (145-610 keV)

Number of iterations = 1

Standard deviation of point of unit weight = 0.00124982157664

R-square (goodness-of-fit statistic) = 0.996085202934

<u>i</u>	Parameter A _i	Std. Dev. A _i
1	0.16187659187	0.00482823092357
2	-6.496720091E-4	4.454643661E-5
3	1.085893015E-6	1.272990093E-7
4	-6.526909298E-10	1.135229486E-10

REGION 3 (610-1400 keV)

Number of iterations = 1

Standard deviation of point of unit weight = 5.921878727E-4

R-square (goodness-of-fit statistic) = 0.96544587054

<u>i</u>	Parameter A _i	Std. Dev. A _i
1	0.107576619786	0.0190544950311
2	-2.40695096E-4	5.700447101E-5
3	2.079626197E-7	5.561226132E-8
4	-6.195007511E-11	1.775279105E-11

ACKNOWLEDGMENTS

I would like to thank Drs. Lyle Roberts and Albert Gudat for their reviews of the draft of this report and their constructive suggestions. I am grateful to D. Rayno for his assistance in preparation of samples and measurement of activity in selected samples using an alpha spectroscopy technique. I am indebted to Claude W. Sill for providing the uranium ore samples. I acknowledge the support of both Leonard Link and Walt Kisieleski during these studies. I would also like to thank Beatrice Grabowski for her meticulous editorial reviews of the manuscript and John DePue for the final preparation of the manuscript.

I am indebted to Dr. Dennis Melodowitch, Application Programming, for preparation of software and to staff of Northland Corporation for technical assistance during these studies.

Distribution of ANL/ES-118Internal:

E.S. Beckjord	M.H. Momeni (50)
L. Burris	D. Rayno
P.G. Chee	C.J. Roberts
P.T. Cunningham	R.E. Rowland
C.A. DeLorenzo	J. Rundo
A.J. Dvorak	J.P. Schiffer
P.R. Fields	J. Sedlet
B.R.T. Frost	A.F. Stehney
A.E. Gudat	M.G. Strauss
W.J. Hallett	R.J. Teunis
E. Huberman	C.E. Till
W.E. Kisielewski	Y. Yuan
J.H. Kittel	ANL Patent Department
L.G. LeSage	ANL Contract File
J.H. Martens	ANL Libraries (2)
	TIS Files (6)

External:

DOE, for distribution per UC-11 (236)
 Manager, Chicago Operations Office, DOE
 President, Argonne Universities Association
 Division of Environmental Impact Studies Review Committee:
 S. Burstein, Wisconsin Electric Power Co.
 J.W. Firor, National Center for Atmospheric Research
 B.M. Hannon, University of Illinois, Urbana
 D.W. Moeller, Harvard University
 H.G. Morgan, Carnegie-Mellon University
 A.F. Smith, University of Michigan
 B.G. Wixson, University of Missouri-Rolla
 G.F. Knoll, University of Michigan,
 D. Melodowitch, Northland Corp., Fort Atkinson, WI
 M. Merritt, Sandia National Laboratory, Albuquerque
 G.E. Miller, University of California, Irvine
 A. Moghissi, U.S. Environmental Protection Agency, Washington
 M.E. Nelson, United States Geological Survey, Albuquerque
 R.W. Perkins, Pacific Northwest Laboratory
 H. Rarrich, Sandia National Laboratory, Albuquerque
 C.W. Sill, EG&G, Idaho
 A.R. Smith, Lawrence Berkeley National Laboratory
 J. Van Allen, University of Iowa
 R. Vaninbroukx, Centraal Bureau voor Nuclearie Metingen van de Europese
 Gemeenschappen, Geel, Belgium
 M.G. White, Office of Nuclear Waste Management, USDOE
 J. Youngerman, University of California, Davis



3 4444 00014640 7

X

